



HAL
open science

Hierarchically porous monolithic MOFs: An ongoing challenge for industrial-scale effluent treatment

Fabrice Lorignon, Alban Gossard, Michaël Carboni

► **To cite this version:**

Fabrice Lorignon, Alban Gossard, Michaël Carboni. Hierarchically porous monolithic MOFs: An ongoing challenge for industrial-scale effluent treatment. *Chemical Engineering Journal*, 2020, 393, pp.124765. 10.1016/j.cej.2020.124765 . hal-03674522

HAL Id: hal-03674522

<https://hal.umontpellier.fr/hal-03674522>

Submitted on 22 Aug 2022

HAL is a multi-disciplinary open access archive for the deposit and dissemination of scientific research documents, whether they are published or not. The documents may come from teaching and research institutions in France or abroad, or from public or private research centers.

L'archive ouverte pluridisciplinaire **HAL**, est destinée au dépôt et à la diffusion de documents scientifiques de niveau recherche, publiés ou non, émanant des établissements d'enseignement et de recherche français ou étrangers, des laboratoires publics ou privés.



Distributed under a Creative Commons Attribution - NonCommercial 4.0 International License

Hierarchically porous monolithic MOFs: an ongoing challenge for industrial-scale effluent treatment

Fabrice Lorignon,^{a,b} Alban Gossard^{b*} and Michaël Carboni^a

^a ICSM, Univ Montpellier, CEA, CNRS, ENSCM, BP 17171, 30207 Bagnols-sur-Cèze
Cedex, France

^b CEA, ISEC, DMRC, STDC, Laboratoire des Procédés Supercritiques et de
Décontamination, Marcoule, F-30207 Bagnols-sur-Cèze, France

*Corresponding author: Alban Gossard

E-mail address: alban.gossard@cea.fr

Phone: +33 4 66 33 91 34. Fax: +33 4 66 79 14 93

Abstract

Metal-Organic Frameworks (MOFs) have attracted a lot of attention over the past two decades mainly because their unique set of properties, notably their high porosity and surface area, are useful for gas storage and separation, but these materials are also well suited to the decontamination of liquid effluents. They are synthesized as crystalline solid powders but, for a broad applicability, producing MOFs as handleable materials is crucial. Furthermore, the main challenge for their use in fix bed processes consists in creating and controlling a meso- and macroporous network in the body of the material while ensuring the MOF's micropores remain accessible. Two techniques have recently been proposed, mechanical shaping and sol-gel synthesis, with the main difficulty in both cases being to retain the properties of the MOFs in the final product, because of the pressure (for mechanical shaping) or the additives (for sol-gel synthesis) required to pack the powder. The focus of recent developments has therefore been on using mild synthesis conditions (sol-gel processes, in situ synthesis, templating). Although relatively few studies have been published to date, the field is expanding fast in terms of the techniques proposed and the understanding of the stability of MOFs and their performance as hierarchically porous materials rather than powders. This review will describe current developments in the shaping of MOFs with an emphasis on the design and control of the final porous structure for effluent treatment applications.

Keywords

Metal-Organic Frameworks; Shaping; Macroporous monolith; Template; Effluent treatment

1. Introduction

Metal-Organic Frameworks (MOFs), hybrid porous organic/inorganic materials, are a class of crystalline molecular solid formed by the self-assembly of organic linkers with metal ions or clusters [1]. These materials offer high porosity, large surface areas and excellent chemical and thermal stability [2]. The wide range of potential linkers and metals allows their structure to be tailored to specific requirements, which has proved advantageous for a wide range of applications such as gas storage [3], heterogeneous catalysis [4], effluent treatment [5], metal separation [6], drug delivery [7] and photocatalysis [8]. Their exceptional properties have increasingly drawn industrial attention toward MOFs rather than other attractive porous materials (activated carbon, zeolites, and silica based materials). Several companies have thus successfully begun the commercial production of MOFs, notably HKUST-1 (Basolite C300, $\text{Cu}_3(\text{BTC})_2$ with BTC= benzene-1,3,5-tricarboxylic acid) and ZIF-8 (Basolite Z1200, 2-Methylimidazole zinc salt) [9]. However, developments over the past two decades in this field have mainly been based on fundamental studies [10] and the nano- or micro-scale of the crystals typically obtained from traditional MOF synthesis reactions (generally solvothermal methods or mechanochemistry [11]) are not necessarily well suited to an industrial scale implementation. The main advantage of embedding MOFs on monolithic supports is thus that it makes them easy to handle and reuse [12]. These features are required to move MOF development forward from academic research to potential industrial applications [13].

Furthermore, while MOFs are mainly used for separation, catalysis and effluent treatment (pollutant adsorption, decontamination), because of their pore size range, powders are not the ideal material form for these applications. For instance, MOFs have shown great promise for the extraction of organic pollutants such as PFOX (aliphatic perfluorinated molecules) [14,15] and BTEX (aromatic hydrocarbon) compounds [5], and for metal extraction [16], but because

of their powder form, experiments have been limited to batch-mode and lab-scale demonstrations. To promote further developments and make them easy to handle, MOFs need to be produced as bulk monoliths. A hierarchically porous structure (micro-, meso-, and macropores) is desirable for the continuous fixed-bed processes used in catalysis and effluent treatment: a macroporous network to improve the hydrodynamic properties of the process (reduce pressure loss) and a micro- and mesoporous network to increase the exchange surface between the active material and the effluent.

The literature is currently lacking in efficient, simple and economic shaping procedures for MOFs that do not alter the material's properties. A number of procedures used to fix powders onto a support have been successfully applied to MOFs. The simplest involves mechanically treating pre-synthesized MOFs [17], a well-established method in the pharmaceutical and agrochemical industries, amenable to 3D printing [18]. Unfortunately, the compacting process drastically reduces the porosity of the powders and is not suited to the shaping of macroporous, or hierarchically porous containing macropores, materials. Other promising techniques include depositing functional MOFs onto monoliths or directly forming monolithic MOFs by emulsion templating. Pore sizes in the monoliths can be tuned from the micro- to the macroscale, which is ideal for effluent treatment.

The objective of this review is to describe the current state of research on shaping MOFs, with a focus on the design and control of the porous structure of the bulk material. The latest developments are summarized in five parts: (i) mechanical shaping, (ii) synthesis of Metal-organic gels, (iii) integration of MOFs into pre-synthesized macroporous structures, (iv) synthesis of host materials around pre-synthesized MOFs, and (v) monolithic MOF shaping from Pickering emulsions. The different synthetic pathways are described to highlight the advantages and drawbacks of each method and outline the directions with the highest potential for shaping MOFs in the future.

2. Mechanical shaping

MOFs are generally synthesized as loose powders via solvothermal processes at specific temperature and solvent conditions, with modulators (molecules that control the reaction kinetics) sometimes added to increase the crystallinity of the materials. They can be shaped into solid materials mechanically by pressing [19], granulation [20], extrusion [21], spray drying [22] and even 3D printing [23]. MOFs have also been deposited as thin films on various substrates [24] by layer-by-layer assembly [25], spin coating [26], coating with a binder-containing MOF suspension [27], and electrochemical deposition [28]. These approaches have mainly been developed for photocatalysis and optical applications since the support can be transparent and conducting [8]. The main difficulties for the development of these devices are that the deposition process needs to be sufficiently reproducible and controllable. These techniques will not be discussed further here, as thin films are not suitable to form the hierarchically porous materials required for gas storage and effluent treatment. Some of the most promising mechanical shaping techniques for these applications are described below.

2.1. Pressing/Granulation/Extrusion

Dry powders are readily compacted into pellets or agglomerated into grains or granules but any crystalline or porous network in the material could be destroyed in the process. It has been shown that the density variations of a packed crystalline powder, due to different strengths of pressing, can change the final properties of the material. By example, packed HKUST-1 (by hand to 5 tons) densities and porosities can differ greatly from those of a fully activated material conducting to a diminution of the functional storage capacity [19].

Wet granulation on the other hand, developed in the pharmaceutical industry to prepare tablets and capsules, agglomerates fine powders into handleable solids without changing their

chemical identity [29]. This method has been used to shape MOFs with binding agents, typically polyvinyl alcohol (PVA) but also sucrose [30], chitosan [20] or silicone resin [27]. MOF granulation is often performed in addition to extrusion [31] or centrifugation [32]. UiO-66, a Zr-MOF based on BDC (benzene-1,4-dicarboxylic acid) has been successfully shaped as a granular material by mixing it with sucrose (10 wt.%) (**Fig. 1a**) [30]. The high porosity and surface area of this MOF make it interesting for gas sorption or separation.

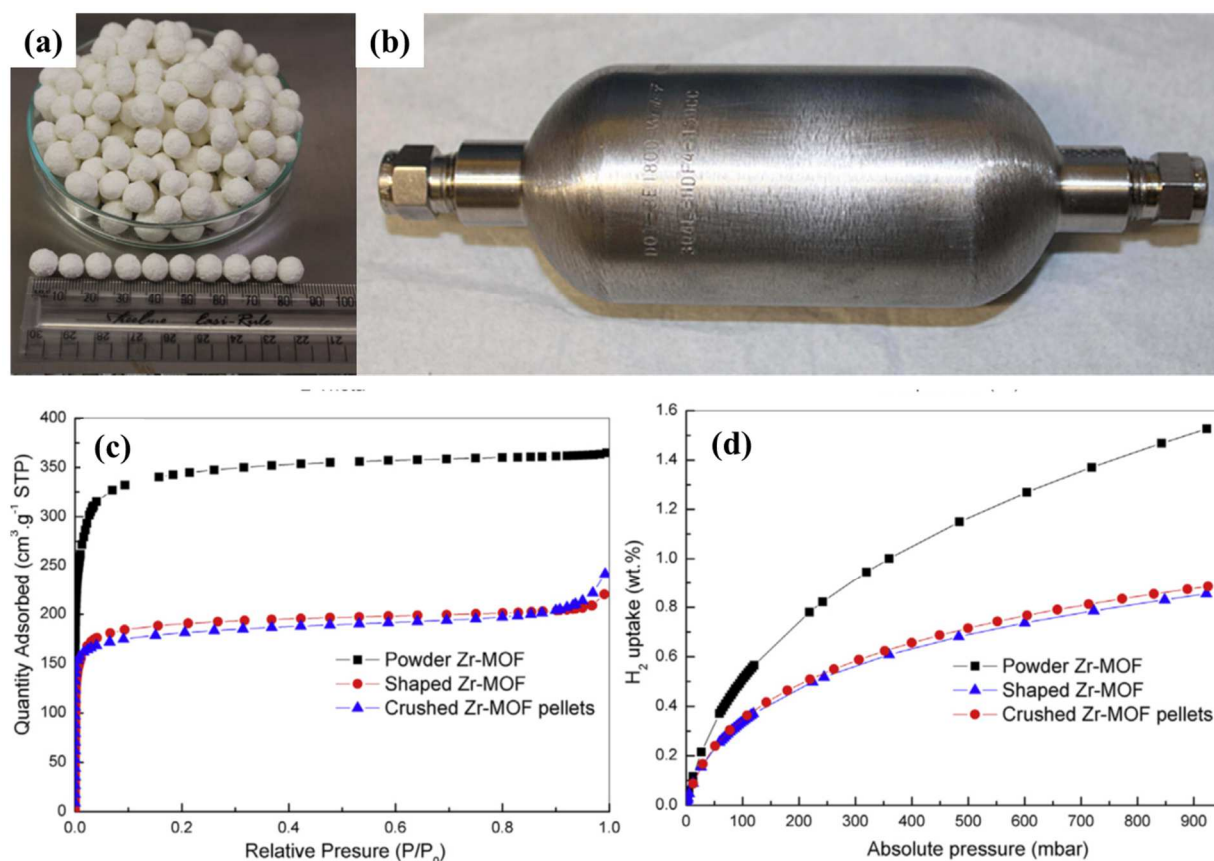


Fig. 1. (a) UiO-66 MOF shaped as spherical pellets with a diameter of about 8 mm. (b) Photograph of a canister packed with UiO-66 pellets. (c) N₂ sorption isotherms and (d) H₂ sorption isotherms at 77 K and 1 bar for UiO-66 as a powder, pellets, and crushed pellets [30].

It has been proposed that the sucrose particles act as bridges between UiO-66 particles, thereby strengthening the MOF network in the pellets. The interparticle macropores between the MOF crystals in the UiO-66 pellets should facilitate mass transport and external diffusion

of hydrogen molecules. The crystal structure of UiO-66 remained intact after centrifugal granulation [30]. As a proof of concept, a canister was packed with 5 mm UiO-66 pellets and N₂ and H₂ sorption isotherms were recorded (**Fig. 1b–d**). The shaped UiO-66 MOFs adsorbed substantially less N₂ and H₂ (**Fig. 1c and 1d**, respectively) than the powder but the sorption capacity of the material was still high and promising for the envisaged application [30].

Choosing the right binder and optimizing its concentration are both crucial to preserve the properties of the MOFs. For MIL-53, a flexible Al-MOF with a heat- and adsorption-dependent structure, this breathing-like behavior is preserved when the MOF is mixed with 13 wt.% PVA [33], but the microporous volume is 32 % lower after shaping because of pore blocking. In contrast, the decrease in pore volume is only 1.5–10.6 % when MIL-53 pellets are produced by extrusion with methyl cellulose as binder [34]. The breathing behavior of the MOF and its high surface area are also preserved, and the CO₂ and methane sorption capacities of the pellets are similar to those of the powder (96 %) [34].

2.2. *Spray drying*

The spray drying procedure, well known in different industrial applications, is a relative new synthesis method that has been first proposed for the synthesis of couple of MOFs [35]. In a typical procedure, the different constituent of the MOFs are prepared in the form of a solution (or slurry) which are then atomized (generally by a nozzle) and dried by a spray dryer to form very small particles. In most cases, a special device with two or three nozzles is required in the spray drying equipment. Nano-sized MOFs can also be used directly in the spray-dryer to pack the MOFs and to form small objects with hierarchical structures and controllable morphologies and sizes [22]. More interesting, this method has been recently used for simultaneous synthesis and shaping of microspherical MOF beads [36]. At this time, this technic can only formed small objects, which limit the application fields.

2.3. 3D printing

Loss of properties (especially the porosity and the crystallinity of the pristine materials) and restrictions on the final shape limit the applicability of mechanically shaped MOFs. The advantage of 3D printing in this context is that complex structural networks can be created directly with much less waste than with other techniques. The paste (ink) is extruded layer-by-layer through a syringe at moderate or ambient temperature [37]. The requirements for the ink are that it should solidify quickly but not aggregate inside the needle of the syringe. As with extrusion/granulation, the formulation of the ink is crucial and, for MOFs, polymeric binders (such as acrylonitrile butadiene styrene (ABS)) have been proposed [38]. MOFs were successfully 3D-printed in this way but their BET surface area was reduced because of pore clogging [38]. Recently, a HKUST-1 gel with printing-friendly rheological properties was shaped directly, without any binders [39]. While the bulk material produced had a lower porosity than the original powder, it was higher than the values obtained using other shaping techniques [39].

The advantages of mechanical shaping techniques are that different geometric shapes can be produced and that the macroporous network and interconnectivity of the pores in the MOFs are predefined and therefore controlled during the preparation of the material. However, these technologies require expensive mechanical and (for 3D printing) computing equipment. A less expensive, direct and popular method to produce MOF monoliths is to use metal-organic gels (MOGs).

3. Metal-organic gels (MOG)

The porosity of crystalline MOF powders depends strongly on the linker-metal pair used. Their microporosity is thus easy to adjust [40,41] by trying different combinations of linkers and metals. For gas treatment, the presence of mesoporous channels improves mass transfer and increases the contact surface between the gas and the MOFs [42].

Meso-microporous MOFs can be produced using sol-gel processes combined with surfactant micelles, as have widely been used to create mesoporous silica oxide structures such as MCM-41 (Mobil Composition of Matter No. 41), and SBA (Santa Barbara Amorphous) [42–44]. Mesoporous HKUST-1 has been synthesized in this way using the surfactant cetyltrimethylammonium bromide (CTAB) as a structural agent [46]. In this approach, the size of the mesochannels depends on the surfactant concentration up to a limit of 5 nm, the diameter of the micelles at the critical micelle concentration [47]. Larger pores have nonetheless be obtained by adding a swelling agent [46], typically a hydrophobic molecule such as tetramethylbenzidine (TMB), which positions in the center of the CTAB micelles during synthesis and increases their size. However, removing bulky molecules such as CTAB and TMB from the channels can be tricky, such that pore blocking is a common problem and a considerable drawback of this approach.

An innovative one-step synthesis of macro-microporous MOFs was reported in 2009 by Kaskel et al. [48]. The photocatalyst and water adsorbent MOF MIL-100(Fe) was synthesized from a mixture of BTC (the linker) in ethanoic solution and $\text{Fe}(\text{NO}_3)_3$ with a 2:3 molar ratio. With this preparation, a MOG is obtained after strong agitation for a few minutes and after drying using supercritical CO_2 (scCO_2), the density of the resulting Metal-Organic Aerogel (MOA) is proportional to the concentration of the linker in the gel (**Fig. 2**) [48]. The potential of using scCO_2 to activate MOFs has also been discussed since it increases the specific

surface area by making more pores free [49]. The structure of the final material depends strongly on the drying process. While a MOA, with an inflated structure, is obtained when the gel is gas-dried (**Fig. 2c**), a much denser lower-porosity Metal-Organic Xerogel (MOX) is obtained after drying by solvent evaporation (**Fig. 2b**) [50,51]. It should therefore be possible to prepare hierarchically porous MOFs, i.e. with MOA or MOX features, by adjusting the drying step.

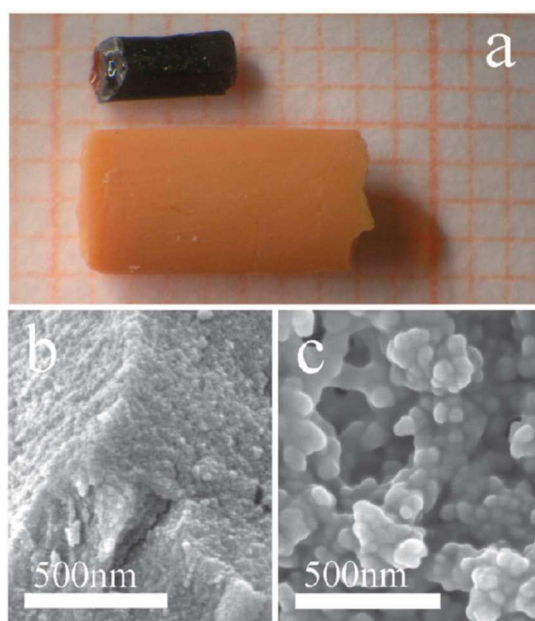


Fig. 2. (a) Photograph of a MIL-100 (Fe) aerogel (orange) and xerogel (black). (b, c) Scanning electron micrographs of (b) a MIL-100(Fe) xerogel obtained after solvent evaporation and (c) a MIL-100(Fe) aerogel obtained after drying in supercritical CO₂ [48].

The gelation mechanism is thus a key part of the process. **Fig. 3** presents the gelation mechanism proposed by Li et al. for the formation of light MIL-53(Al) meso-microporous aerogels from aluminum nitrate and BDC in a DMF/EtOH solution [52].

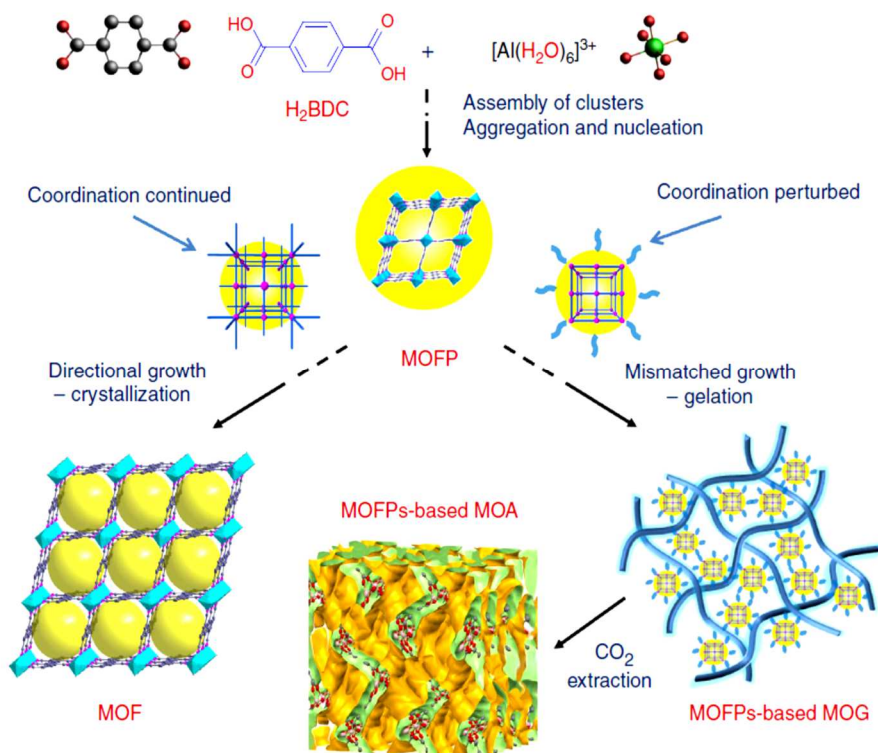


Fig. 3. Schematic representation of how an Al(BDC) Metal-Organic Gel is obtained instead of a crystalline Metal-Organic Framework (MIL-53(Al)). BDC, benzene-1,4-dicarboxylic acid; MOFP, Metal-Organic Framework Particle [52].

The first step is the self-assembly of strong linker–metal clusters ($\Delta H_{298} = 512 \text{ KJ}\cdot\text{mol}^{-1}$ for the Al-O bond). The aggregates obtained gradually polymerize in the nucleation phase. In the second stage, the balance of competitive interaction forces induces either gelation or continued crystallization (**Fig. 3**). Temperature is the key parameter to disrupt the coordination balance. Mild heating promotes the reversibility of the coordination bonds, which become weak and comparable to other interactions (H-bonding, π - π stacking, hydrophobic effects and van der Waals interactions). These supramolecular forces disrupt crystallization and precipitation, promoting the self-standing monolith synthesis [52]. The gelation process also depends on the heating time. New Al(BDC) patterns appear when the aggregates are heated at 50–60 °C for more than 80 min, promoting gelation over

crystallization. Many different MOGs have been prepared in this way, by varying the heating time and temperature [46,48,50,53,54].

Chemical parameters, such as the metal source and reagent concentrations, also have a strong effect on gelation. Bueken et al. noticed that gelation was easier to achieve with $\text{ZrOCl}_2 \cdot 8\text{H}_2\text{O}$ than with ZrCl_4 , as expected since $\text{ZrOCl}_2 \cdot 8\text{H}_2\text{O}$ is a hydrolysis product of ZrCl_4 and its more advanced oxidation state makes it less reactive with water. It is also a direct precursor of the zirconium cluster $[\text{Zr}_6\text{O}_4(\text{OH})_4]^{12+}$ in UiO-66 [54]. This study highlights the importance in this process of water, which influences the hydrolysis rate of the zirconium salts and therefore the gelation step. Gelation is promoted when the solutions contain metal ions from different sources, and the fact that each metal species reacts differently needs to be considered carefully when designing the gel. Each metal nature moiety coordinates differently with the linker in various conditions, preventing total crystallization. The mixed MOG Al/Fe(BTC) is an example of the materials obtained [55]. BTC coordinates with Al at high temperature (120°C) but coordinates preferentially with Fe at room temperature [56]. In addition, the pore volume in the MOG depends on the relative concentration of the metal species, with a maximum volume of $9.7\text{ cm}^3 \cdot \text{g}^{-1}$ observed for equal molar ratio 0.5Fe-0.5Al-BTC [55]. The final means to promote gelation is to increase the reagent concentration, leading to viscous gel with aggregated weakly linked particles [54]. **Fig. 4** shows a schematic overview of the different scenarios described above as well as the effects induced and the resulting microstructures.

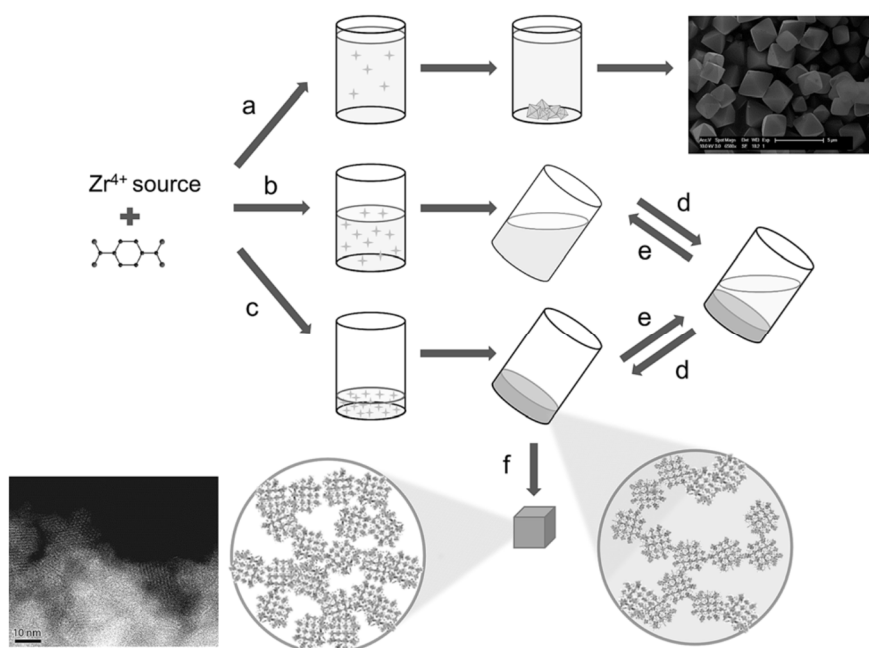


Fig. 4. Schematic overview of Metal-organic gel formation: (a) under dilute conditions, (b) under intermediate conditions, (c) at high particle concentrations, (d, e) with mechanical stimulation and (f) after solvent removal [54].

Recently, Fairen-Jimenez *et al.* demonstrate the critical importance of different parameters to obtain a robust and dense (and microporous) monolith from a MOF (HKUST-1 and Zr-UiO-66)-containing gel [57,58]. Primary particles forming the gel have to be small and grow at the gel interface during drying to maintain the monolithic shape. Then, the drying step has to be slow and performed in mild conditions. Indeed, a too fast drying of the gel induces a collapse of the 3D structure due to the mechanical stress created by the meniscus at the vapour-liquid interface during the solvent evaporation. These works underline once again the importance of the temperature in such processes. Such monoliths exhibit remarkable methane adsorption capacities. Furthermore, by finely adapting the drying conditions, the authors are also able to create mesopores between primary UiO-66 particles, which significantly improve the material performance due to the gas condensation in the mesoporosity [58].

As mentioned in the introduction, to be used in industrial fixed bed reactors, MOFs designed for catalysis and separation processes have to be monolithic and hierarchically porous. A high specific surface area is required to maximize their exchange capacity (efficiency), and a connected macroporous network is required to improve fluid (liquid or gas) transport and avoid pressure drop during the process. The following section discusses the latest research on the synthesis of hierarchically porous monoliths containing MOFs.

4. Integrating MOFs in a pre-synthesized macroporous support

Using a pre-synthesized “host” macroporous support is an interesting approach because the macroporous structure and the shape of the material can be determined in advance and adapted to the desired application. Macroporous supports can be purchased or manufactured in house; MOFs are generally impregnated into the macroporous structure or synthesized in situ. Commercial monolithic alumina supports with different macropore sizes (respectively on the millimeter and hundred nanometer scale) have thus been used as hosts for MIL-101(Cr), a MOF based on BDC, for catalysis [59], and for HKUST-1 to design membranes for small-molecule separation [60]. Impregnation was achieved in two stages: a single seeding step in which the alumina support was immersed in a suspension containing pre-synthesized MIL-101(Cr) [59] or several cycles of immersion in BTC and Cu^{2+} precursor solutions [60], followed by hydrothermal treatment in a MOF precursor solution, as a secondary growth, to ensure the macropores are uniformly coated with MOFs. Both stages are important. Without seeding, the MOFs tend to grow in the precursor solution during the hydrothermal treatment and do not well attach well to the internal surface of the macropores [59]. The second stage is essential to improve the homogeneity of the MOF layer, notably by increasing the precursor concentration.

HKUST-1 MOFs have also been incorporated into hierarchically porous carbon monoliths (synthesized by pyrolyzing an initially polymeric monolith) by step-by-step impregnation and hydrothermal crystallization [61]. This process was repeated twice to achieve 17 % occupancy of the monolith's pore volume by the MOFs. These materials have high CO₂ uptake capacities, which increase with their MOF content. Moreover, the MOFs synthesized in situ are smaller than those obtained by “free” synthesis (i.e. without the porous carbon monolith) because of steric hindrance from the carbon skeleton [61]. The size of the MOFs can thus be tuned by varying the size of the macropores in the monolith.

Betke et al. have investigated the effects of the polarity of the internal surface of the macroporous material and its microstructure (roughness, pore size) on the deposition of four MOFs (HKUST-1, CAU-10 (an Al-based MOF with BDC), MIL-101(Cr) and UiO-66) [62]. Commercial SiC foams and pre-synthesized alumina foams were silanized using APTES, to produce nonpolar surfaces (from the presence of alkyl chains), and then further modified with terephthaloyl acid (COCl) to produce polar surfaces (from the presence of COOH groups after COCl treatment). The monolithic macroporous supports were coated by direct crystallization in hydrothermal conditions in the presence of precursors specific to the targeted MOFs. Betke et al.'s study demonstrates that the effects of the surface of the support depend on the nature of the MOF. For HKUST-1, there was no significant difference in deposition after surface treatment and the coating efficiency was mainly affected by the surface roughness of the support. The best results were obtained with the rougher SiC foam, whose larger specific surface area offers better mechanical anchoring possibilities for HKUST-1 particles. On the contrary, the coating efficiency with CAU-10 improved after COCl treatment, showing that it depends on the surface chemistry of the substrate rather than its morphology. The hydroxy groups act as seeding points for the growth of MOF particles on the surface. Reducing the number of COOH groups on the surface led to the growth of fewer but larger MOF particles.

With MIL-101(Cr) and UiO-66, the same fine layers of small particles (respectively 200 nm and 50 nm in diameter) were deposited on both substrates regardless of how they were treated [62].

Metal-organic frameworks have also been inserted in silica monoliths [63,64]. Hierarchically porous silica has indeed widely been used for many years as a host matrix for various fixed bed applications [65]. As reported first by Sachse et al. for continuous flow catalysis [63], the silica monoliths used in these studies [63,64] were prepared by spinodal decomposition to create interconnected 5 μm macropores (**Fig. 5c**), and a mesoporous network was formed by alkaline treatment. HKUST-1 particles were impregnated using a solution of $\text{Cu}(\text{NO}_3)_2$ and BTC in DMSO followed by crystallization induced by solvent evaporation. The **Fig. 5a** presents an image of the HKUST-1-impregnated silica monolith. The blue color is characteristic of the presence of copper in the material and the **Fig. 5b** demonstrates the homogeneity of the impregnation.

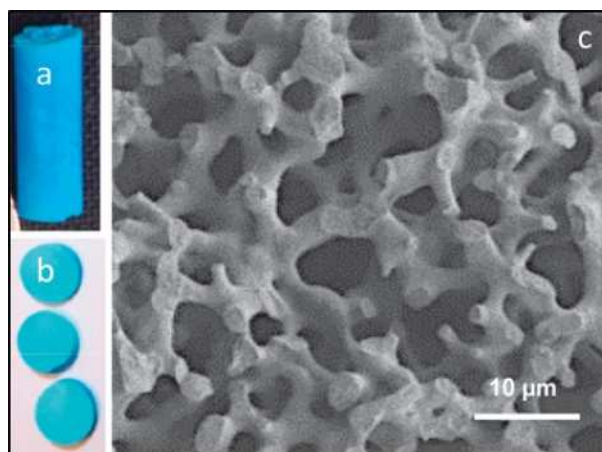


Fig. 5. (a) and (b) Photographs of a hierarchically porous silica monolith impregnated with HKUST-1 particles. (c) Scanning electron micrograph of the monolith [63].

Scanning (**Fig. 5c**) and transmission electron microscopy showed that the majority of the HKUST-1 particles were embedded inside the mesopores of the monolith and would thereby not hinder flow through the macroporous network. The material catalyzed a Friedländer

reaction between 2-aminobenzophenone and acetylacetone under continuous flow more efficiently than a commercial HKUST-1 powder did in batch experiments. A few years later, Song et al. used a similar synthesis to study the influence of the MOF precursor concentration on the size and location of the MOF particles in the pores of the monolith [64]. The deposited HKUST-1 particles were larger and located in the macropores of the monolith (rather than in the mesopores) when a higher-concentration MOF precursor solution was used. The use of polymeric foams as hosts materials for MOFs was demonstrated for the first time in 2008 by Schwab et al., who integrated HKUST-1 in a monolithic macroporous hydrophilic polyHIPE [66]. PolyHIPEs are macroporous foams obtained by polymerization of the continuous phase of an emulsion generally stabilized using surfactants. A monolithic solid skeleton forms around the emulsion droplets that when removed, leaves behind a network of interconnected macropores. In Schwab et al.'s study, polyHIPEs were obtained by polymerizing 4-vinylbenzyl chloride cross-linked with divinylbenzene in a water-in-oil emulsion stabilized with the commercial nonionic surfactant Span 80 [66]. The internal phase was removed by Soxhlet extraction and, after hydrophilizing the internal walls of the polyHIPEs, HKUST-1 crystals were grown inside the (micron-scale) macropores of the polyHIPE in several cycles of precursor impregnation and hydrothermal treatment (**Fig. 6a**).

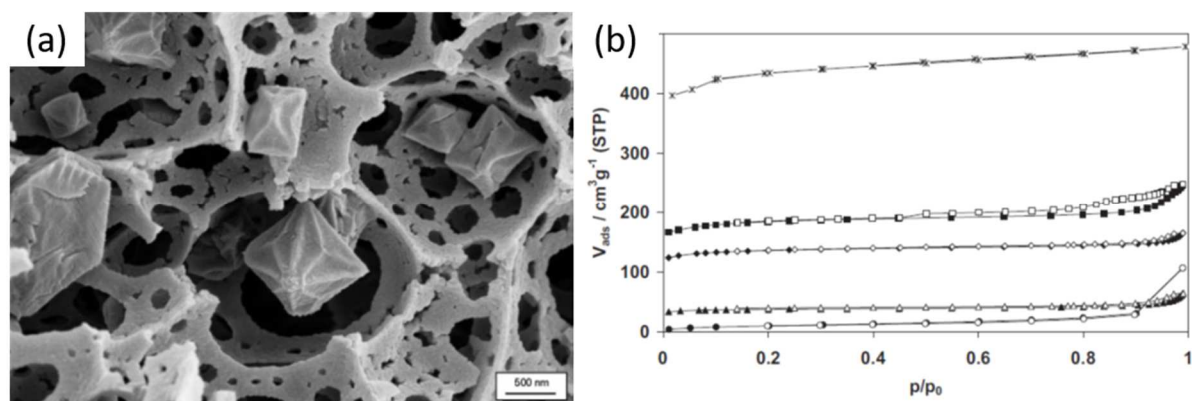


Fig. 6. (a) Scanning electron micrograph of HKUST-1 MOF particles embedded in a polyHIPE. (b) N₂ adsorption and desorption isotherms (respectively solid and empty

symbols) of HKUST-1@polyHIPE after successive impregnation cycles: no impregnation (circles), one impregnation cycle (triangles), two impregnation cycles (diamonds) and three impregnation cycles (squares). The stars show the isotherm measured for pure HKUST-1 [66].

A crucial feature of the polyHIPE's macroscopic structure is that it survived the hydrothermal treatment, allowing three successive impregnation steps. **Fig. 6b** shows the adsorption and desorption isotherms measured after each impregnation step. Each step increased the BET surface area and the number of micropores, demonstrating additional MOF growth and macropore filling. This work paved the way for a number of studies in different fields such as organic vapor adsorption [67] and dye removal [68].

In Wen et al.'s layer-by-layer approach [69], the internal surface of a pre-synthesized macroporous polymer is first functionalized and repeated impregnation of zirconium salts leads to the progressive and homogeneous growth of a ZIF-8 layer. This strategy offers precise control over the thickness of the deposited MOF layer, preserving the transport properties of the original polymeric monolith, especially its permeability.

Natural products, such as cellulosic compounds, have attracted growing interest in recent years as alternatives to synthetic materials, particularly polymeric foams. Furthermore, the presence of hydroxyl groups on their surface makes them easy to functionalize. Monolithic macroporous cellulose based-aerogels have been impregnated in this way with different types of MOFs [70,71]. MOFs such as ZIF-8 and UiO-66 can be grown on monolithic bacterial cellulose aerogels [66]. The surface hydroxyl groups ensure good adsorption of the metal ions through weak interactions, and the metal ions then act as anchor sites for MOF growth. The mechanical properties of the cellulose-based materials are also interesting, particularly their ductility and flexibility. These properties are retained after MOF growth such that the final

material combines the lightness, macroporosity and flexibility of the cellulose skeleton with the high porosity and functionality of the MOFs.

The integration of MOFs by impregnation or in situ synthesis in a monolithic support has particularly been used to develop innovative membranes. Indeed, the fine design of a membrane morphology and porosity is a key point to increase the material performances. Moreover, the membrane support has to present satisfying mechanical properties and an important durability. In this way, MOFs have been embedded into ceramic or polymeric support for application such as gas separation [72–74] or small-molecule removal [60,68] .

The use of pre-synthesized MOF host materials has led to the development of a wide range of composite materials. This approach allows the porous structure of the final material to be designed in advance and a various MOFs can be inserted. However, the limitations of these processes include their complexity ~~due to the~~ (they involve ~~numerous~~ many steps) ~~in the methodology~~ and the fact that the attachment and dispersion of the MOFs in the structure is difficult to control and optimize. Pore clogging can also occur during impregnation and the host materials have to be sufficiently resistant to survive the MOF synthesis conditions. This is why methods in which the host material is assembled around pre-synthesized MOFs or synthesized simultaneously with the MOF appear attractive.

5. Host materials formed around pre-synthesized MOFs

Host materials can be created around MOF particles simply by conventional sol-gel synthesis, typically of silica aerogels [75,76]. MOF particles are first suspended in a solution of silica precursors (typically TEOS) and after hydrolysis and condensation, respectively in acidic and alkaline solutions, and solvent removal, a monolithic mesoporous silica aerogel containing microporous MOF particles is obtained. Nuzhdin et al. have slightly modified this approach to

avoid the MOF micropores becoming blocked in the process [77]. Adding the MOF particles after the hydrolysis and condensation steps (but before gelation) avoids any penetration of the SiO₂ sol into the micropores of the MOF. This protocol ~~can be~~ also be used with polymeric xerogels as the host material [78]. In Wickenheisser et al.'s study, MOFs were added at up to 77 wt.% without any loss of mechanical stability, and adding the MOFs into a pre-polymerized solution avoided any clogging of the MOF micropores. However, the MOF suspension became difficult to homogenize if the pre-polymerization time was too long [78]. These methods are amenable to various MOFs (HKUST-1 [75,79], ZIF-8 [76], MIL-100(Fe,Cr) [78]) with loadings of up to 30 wt.% without any degradation of the monolithic structures. Nevertheless, their applicability in fixed-bed processes remains limited because they lack the macroporous network required to improve fluid transport properties through the material, particularly for liquid effluent treatment. Variants of this approach have therefore been developed with a sacrificial template that ~~will~~ induces ~~a~~ the desired macroporous network.

Templating is generally used in material science to model a porous structure on a particular design (a replica of the template). Among the many possibilities, ice-templating can be used to produce highly interconnected macroporous materials. Ice-templating involves freeze-drying an aqueous solution containing linkable compounds that create a mechanically stable 3D network. The macropores are formed when the ice crystals are removed by freeze-drying. Macroporous monolithic materials with up to 50 wt.% MOFs have been produced in this way by incorporating pre-synthesized MOFs in the initial mixture [80–82]. Fu et al. used chitosan as a polymeric support for UiO-66 particles [80]. These were suspended in water in the presence of chitosan powder and freeze dried, and the monolithic materials obtained were used to extract organic products from water. However, the alkaline treatment used to increase the stability of the material in water degraded the chitosan support, leading to the loss of many

of the embedded MOF particles and a substantial decrease in the porous volume of the material (collapse of the macropores). This process has also been used with cellulose-based materials and different types of MOFs (UiO-66 [81,82], ZIF-8 and MIL-100(Fe) [83]), highlighting its versatility. UiO-66 has been incorporated into a nanocellulose network by self-crosslinking to create flexible and hierarchically (macro-micro-) porous materials with a very low density [82]. The electrostatic interactions between cellulose nanofibers and UiO-66 ensure the UiO-66 particles adhere strongly and limit their aggregation. These materials had good adsorption properties when immersed in contaminated solutions (dyes) and no release of UiO-66 was observed [82]. This is because the formation after freeze-drying of hydrogen bonds between the Zr-OH sites of UiO-66 and the hydroxyl groups of the cellulose minimizes particle leaching. Adding carboxymethyl cellulose (CMC) to the suspension has been shown to increase the mechanical robustness of the monoliths, especially at high MOF concentrations [83]. Mesopores are also formed between the crosslinked nanocellulose and CMC.

Macroporous networks can also be created in monolithic materials by phase separation (generally induced by organic agents such as surfactants or polymers) combined with a sol-gel or polymerization reaction. This method leads to the formation of an interconnected network of pores generally smaller than 20 μm that replicate the separated phase in the solid network. This method has been used to synthesize different oxide and (oxy)hydroxide monoliths [84–86] and the materials obtained can be treated for specific applications in catalysis or liquid effluent treatment [87–89]. However, phase separation is a very sensitive technique and the reaction kinetics often have to be adjusted very precisely to simultaneously induce gelation (or polymerization) and phase separation. Moitra et al. used this approach to synthesize copper oxy(hydroxide) macroporous ($\sim 3 \mu\text{m}$ pore size) monoliths, which were then impregnated with BTC to form HKUST-1 monoliths by pseudomorphic replication [90]. The

polyacrylamide (PAM) used for the phase separation process also showed a surprising ability to stick the (oxy)hydroxide Cu-based colloids together and strengthen the monoliths. These materials are highly crystalline and have a large surface area and good mechanical properties. They can be used as an adsorbent for wastewater treatment, especially for dye removal [91]. MOF monoliths have also been synthesized by phase separating the hydrophilic polymer PVA, used as a MOF binder, and acetone [92]. Acetone was added as a non-solvent additive to a homogenized mixture of PVA and suspended MOFs (commercial Basolite A520 or pre-synthesized MIL-101(Cr)) to induce phase separation, leaving behind a macroporous network after washing. Monoliths loaded with up to 80 wt.% MOFs and macropores between 0.4 and 9.4 μm were obtained [92].

Another commonly used templating approach consists in stabilizing emulsions containing precursors in the continuous phase. Macroporous monolithic materials can be obtained by controlling the growth of the structural material (by polymerization or sol-gel reaction) and removing the internal phase [93–96]. A versatile approach to synthesize these materials consists in using high internal phase emulsions (HIPEs) stabilized with organic surfactants as templates, as the size and interconnectivity of the macropores and the shape of the final monoliths can be adjusted [93–96]. Materials synthesized in this way have been used as supports for MOF impregnation and in situ synthesis, as described above [66]. However, pristine MOFs can also be introduced directly into the emulsion to simplify the process down to a single step, as developed by Janiak and coworkers [97,98]. Three pre-synthesized MOFs from the “MIL family” were introduced into cyclohexane-in-water emulsions stabilized with commercial surfactants and containing polymeric precursors in the continuous phase to produce MIL-MOF@polyHIPE after curing, washing and drying, either with MIL-101(Cr) for vapor adsorption (**Fig. 7a**) or MIL-100(Fe), MIL-100(Cr) or MIL-101(Cr) for water adsorption applications. Scanning electron micrographs of the synthesized materials reveal the

alveolar and interconnected microstructure of the porous network formed by the surfactant-stabilized HIPE template, with macropores a few microns across and pristine MOFS (**Fig. 7b and c**). The MOF agglomerates adhere to the inner surfaces of the macropores with unchanged particle size. The uniform color of the materials indicates that the MOFs are homogeneously distributed on the macroscopic scale, even if this is not always the case on the microscopic scale (inside the macropores) [97]. The MOF concentration has no significant influence on the macropore size, which is generally imposed by the oil volume fraction and the amount of surfactant amount in the emulsion formulation [93–96].

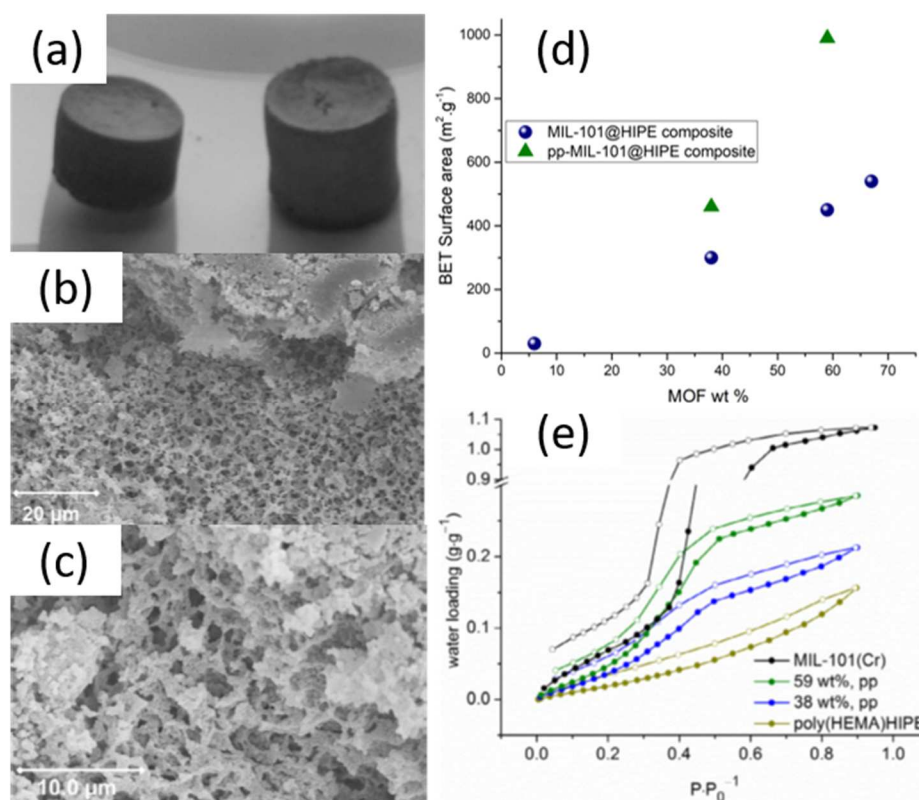


Fig. 7. (a) Photograph of monolithic MIL-101@polyHIPE composites with 38 and 59 wt.% MIL-101. (b, c) Scanning electron micrographs of the MIL-101@polyHIPE composites with (b) 38 and (c) 59 wt.% MIL-101. (d) BET surface area of different MIL-101@polyHIPE composites synthesized either with (triangles) or without (circles) pre-polymerization, as a function of the MIL-101 weight content. (e) Water sorption isotherms measured for pure polyHIPE, pure MIL-101(Cr) and MIL-101@polyHIPE composites with 38 and 59 wt.% MIL-101 synthesized with pre-polymerization [97].

Although this protocol produces monoliths with MOF loading fractions of up to 92 wt.%, the maximum sustainable MOF content depends strongly on the polymeric formulation used [97,98]. Composites can become brittle when the MOF concentration is too high [97], although no clear information has been published on the mechanical properties of these materials. Furthermore, a considerable drawback of this method is that the micro- and mesopores in the MOFs tend to become clogged with HIPE monomers. This effect can be limited by ~~starting polymerize~~ initiating the polymerization of the continuous phase before introducing the MOFs. **Fig. 7d** shows that the BET surface areas of MIL-101@poly HIPE composites increase with the MOF loading fraction and is considerably higher in the composites synthesized with pre-polymerization [97]. Pre-polymerization thus improves the accessibility of the MOFs in the composite. Its effectiveness depends on the polymerization reaction progress and the size of the micro- and mesopores in the MOF. Indeed, smaller pores are more difficult to protect against pore blocking than larger pores are because of higher capillary condensation forces [98]. These materials can be used for water adsorption: **Fig. 7e** shows that the water adsorption capacity increases with the MOF loading fraction when pre-polymerization ensures that the MOFs remain accessible.

Using a surfactant-stabilized emulsion as a template to prepare macroporous monoliths allows the composition of the final material to be adjusted by choosing the right precursors in the continuous phase. However, the MOF particles are embedded in the walls of the macropores, limiting their accessibility for the treated effluent. Pore blocking can occur and the MOF particles can become degraded when the surfactants are removed. In addition, the macropores in surfactant-stabilized emulsions are generally too small for fixed-bed liquid effluent treatment. In contrast, Pickering emulsions are directly stabilized by the particles, without surfactants, and generate bigger droplets and larger macropores when they are used as templates.

6. MOF monoliths from Pickering emulsions as templates

A Pickering emulsion is an emulsion stabilized by solid particles whose interfacial activity is high enough for them to be adsorbed at the interface of two immiscible fluids, reducing the interfacial tension between them and acting as emulsifiers [99,100]. The wettability of these particles, characterized by their contact angle at the oil-water interface (estimated on the aqueous side), determines whether oil-in-water, water-in-oil or more complex (multiple) emulsions are formed. Particle adsorption is strongest and the emulsions most stable when the contact angle is close to 90° (i.e. when the particles are equally wettable by the two phases) [99–102]. Particles typically have lower interfacial activities than surfactants do, which explains why the droplets in Pickering emulsions are larger than those in surfactant-stabilized emulsions.

Stabilizing Pickering emulsions using MOF particles is therefore an attractive approach to form hierarchically porous MOF-containing materials. The adsorption of MOF particles at the oil-water interface should leave them positioned at the surface of the macroporous channels in the monoliths. As mentioned above moreover, the stabilization of larger droplets and the correspondingly larger macropores in the final material should promote faster hydrodynamic transfer.

6.1. Pickering emulsions stabilized by MOF particles

The amphiphilicity of MOF particles means that they can stabilize emulsions without organic surfactants [103]. One of the first demonstrations of MOF-stabilized Pickering emulsions was the use of HKUST-1 particles to stabilize both oil-in-water and water-in-oil emulsions, phase inversion being governed by the oil volume fraction [104]. The HKUST-1 particles gradually reduced the interfacial tension between water and oil from an initial value of $15 \text{ mN}\cdot\text{m}^{-1}$ to 7

$\text{mN}\cdot\text{m}^{-1}$ after 20 min, reflecting dynamic adsorption at the interface. This effect was also observed with CPO-27 MOFs (Ni or Co based MOFs with 2,5-dihydroxyterephthalic acid) [104]. Their interfacial properties mean that MOFs can also be used to stabilize gas-liquid and ionic liquid-liquid emulsions: $\text{Mn}_3(\text{BTC})_2$ and $\text{Ni}_2(\text{BDC})_2$ have respectively been shown to stabilize CO_2 -in-water [105] and [BMIm]PF₆-in-water or water-in-[BMIm]PF₆ emulsions ([BMIm]PF₆=1-Butyl-3-methylimidazolium hexafluorophosphate) [106].

Pickering emulsions stabilized with MOFs are also being investigated as a means to prepare colloidosomes (or MOFsomes, hollow microcapsules) for heterogeneous catalysis and drug delivery [107–109]. The droplets in Pickering emulsions can self-assemble into semi-permeable shells that can be used to protect or deliver cargo molecules. The properties of the organic linker in MOFs can be tuned to modify the hydrophobicity of their surface. This in turn affects the wettability of the MOF particles and determines the area occupied by the two phases on the surface of the particles [110]. These properties can be exploited in the synthesis of MOF-containing porous materials to control the distribution of MOF particles on the surface and inside the pores.

6.2. Macroporous monoliths containing MOFs synthesized from Pickering emulsions

Pickering emulsions can be used just like HIPEs as templates for the synthesis of porous materials. The properties of the resulting monoliths can be adjusted by varying the volume fraction of the phases, the MOF concentration and the shearing rate used to form the initial emulsion.

The high stability of UiO-66 particles in organic solvents allows them to stabilize oil-in-water emulsions of dodecane, hexane, toluene and cyclohexane [111] whose viscosity increases with the oil volume fraction. Average droplet sizes typically decrease when the oil (internal phase) volume fraction increases [106,111,112]. The rheological properties and the average

droplet size of the emulsions also depend on the UiO-66 concentration: about 1 wt.% UiO-66 particles is required to stabilize the cyclohexane-in-water system while above 5 wt.% UiO-66, the emulsions become more viscous and stable against creaming [111]. The droplet size in these emulsions finally depends on the shear rate used during emulsification, with higher shear rates producing smaller droplets [93]. These parameters will all affect the macropore size, the interconnectivity and the density of the final material. Two methods have been proposed to form monoliths from these emulsions: emulsion drying to prepare aerogel-type monoliths and polymerization to prepare polymer-supported monoliths.

6.3. Aerogel-type hierarchically porous monoliths

As in traditional sol-gel synthesis, rapidly drying a MOF-stabilized Pickering emulsion leads to the formation of a MOA. Since the continuous phase is a suspension of MOFs, the channels and walls of the final aerogel are entirely composed of MOFs. The first studies of MOF aerogels from Pickering emulsions were carried out by Zhang et al. with HKUST-1 nanoparticles, $\text{Mn}_3(\text{BTC})_2$ nanowires and $\text{Ni}_2(\text{BDC})_2$ nanosheets [112]. The shape of the droplets in the emulsion depends on the morphology of the MOF particles and as mentioned above, the size of the droplets depends on the oil volume fraction [106]. Photographs of HKUST-1 oil-in-water Pickering emulsions with different oil concentrations are presented in **Fig. 8a–c**. **Fig. 8d** shows how the droplets generate the macropores in the MOA after drying (using scCO_2 and by freeze-drying successively), while the interconnected MOF particles create a mesoporous network that increases the total porosity of the material. However, the mechanical strength of these aerogels is lower than that of other MOF containing materials. The mechanical properties were compared by measuring the Young's modulus of the monolith. These moduli are obtained by uniaxial compression and are representative of the monolith's stiffness. While their Young's modulus increases with the volume fraction of the

continuous phase, Zhang et al. measured values below 34 KPa whereas compressed powder and polyacrylamide supported MOFs have Young's moduli of 445 KPa and 1.5 MPa, respectively [112].

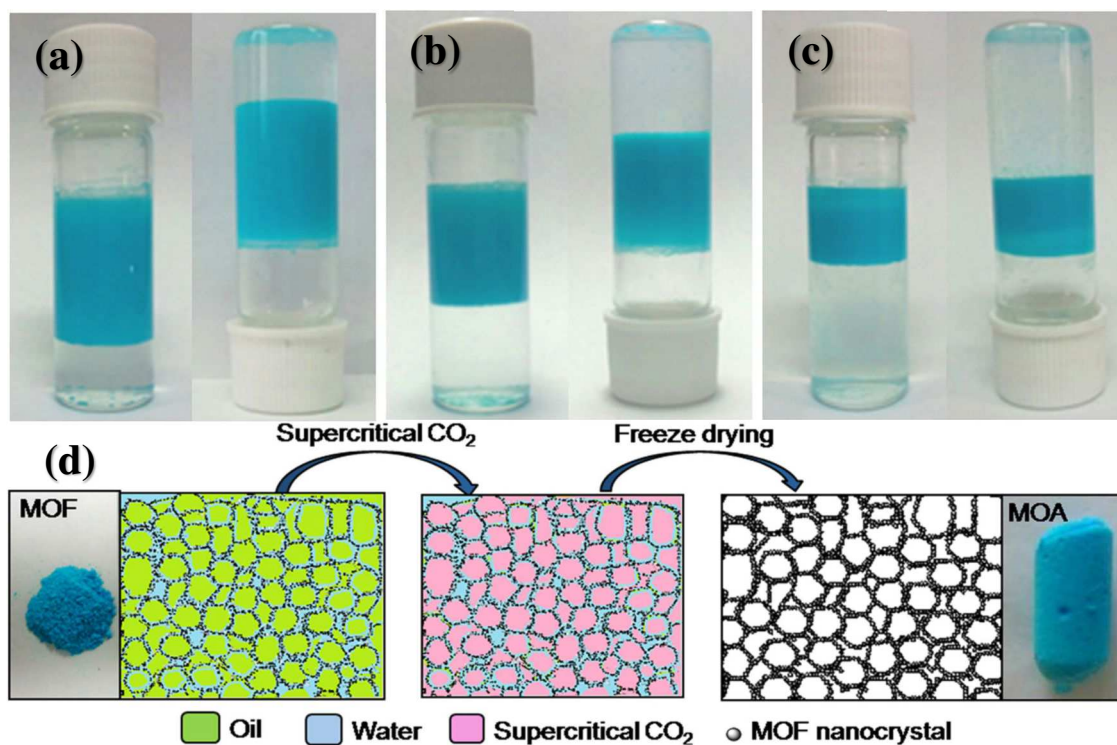


Fig. 8. (a–c) Photographs of Pickering emulsions stabilized by HKUST-1 particles with initial diethyl ether volume fractions of 0.57, 0.43 and 0.29, respectively. (d) Schematic representation of a MOF-stabilized high internal phase emulsion and the process used to obtain a metal-organic aerogel [112].

Pickering emulsions can also be stabilized using MOF-based composites. Zhang et al. prepared a Zr-BDC-NO₂/GO (graphene oxide)-stabilized cyclohexane-in-water emulsion with a 1:1 water-oil volume ratio by sonication [113]. The porous “superstructure” produced after freeze-drying contained MOF particles supported by GO walls. These composites are also brittle however, and for applications such as effluent (particularly liquid) treatment under continuous flow, a higher mechanical strength is required to resist pressure drops. Polymer supported MOFs are typically stronger so one possibility is to add polymer precursors during the emulsification process to polymerize the continuous phase of the emulsion.

6.4. Polymer binders in MOF-stabilized Pickering emulsions

Zhu et al. have investigated the effects of adding a polymer binder to enhance the mechanical resistance of monoliths produced from UiO-66–stabilized Pickering emulsions (0.8 v/v cyclohexane and 5 wt.% UiO-66) [111]. PVA was introduced at 1 wt.% in the aqueous phase which also contained monomer acrylamide, the cross-linker MBAM (N,N'-methylenebisacrylamide) and the initiator $K_2S_2O_8$. These polyacrylamide (PAM) precursors are water-soluble and were added before emulsification shearing. The emulsion was then polymerized by heating the gel at 60 °C and the resulting MOF/PVA monoliths were freeze-dried to remove the solvents. **Fig. 9a** highlights the ultralow density ($15 \text{ mg}\cdot\text{cm}^{-3}$) of the monoliths and the SEM image in **Fig. 9b** shows how the microstructure of the monoliths mirrors the arrangement of the droplets in the emulsion. **Fig. 9c and d** shows the PAM walls of the macropores covered with UiO-66 particles.

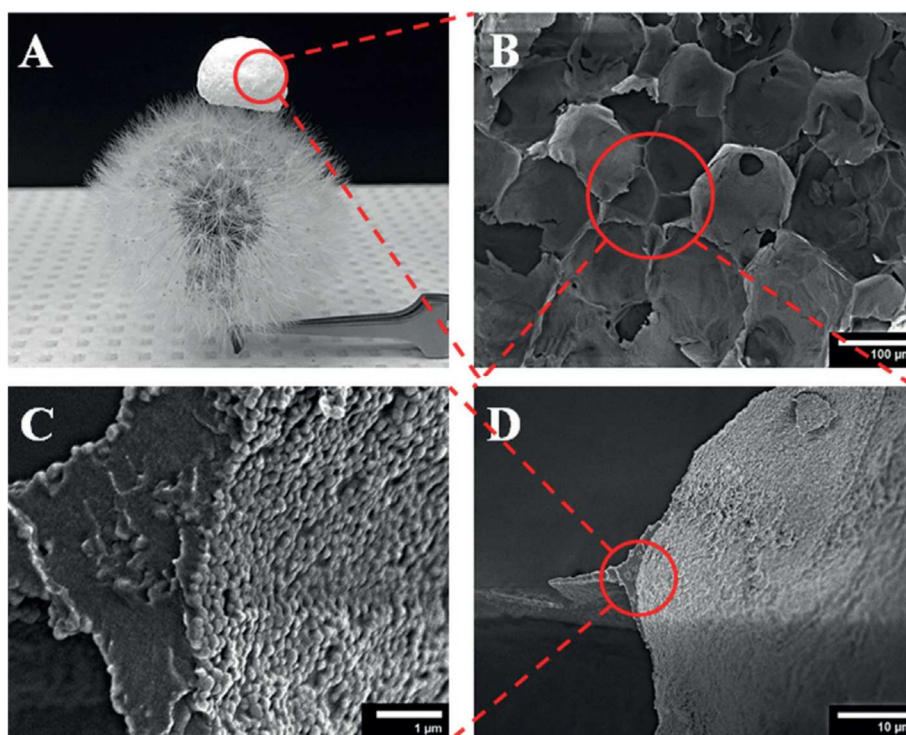


Fig. 9. (a) Photograph of a MOF/polyvinyl alcohol (PVA) porous monolith on a dandelion flower head. (b–d) Scanning electron micrographs of a MOF/PVA porous monolith. The monolith was prepared from a Pickering high internal phase emulsion with a 0.8 v/v cyclohexane internal phase stabilized by 5 wt.% UiO-66 particles and 1 wt.% PVA in the aqueous phase [111].

Adding PVA significantly reduces the size of the oil droplets however, from 151 μm to 29 μm on average. Indeed, PVA acts both as an emulsion co-stabilizer and an adhesive between UiO-66 particles. As a co-stabilizer, PVA reduces interfacial tension, leading to the formation of smaller droplets. The presence of PVA in the aqueous phase increases its viscosity and brings the UiO-66 particles closer together. Wang et al. found that the mean pore diameter in the monoliths decreased from 95 to 33 μm when the PVA concentration was increased from 0 to 3 wt.% in the continuous phase [114]. A final effect of PVA is that it increases the interconnectivity of the porous network, with Wang et al. reporting more closed cells in PVA-free UiO-66/PAM monoliths than in those containing PVA [114].

This MOF@Pickering-polyHIPE strategy using PAM as a wall and PVA as an adhesive has also been used for CO₂-in-water foams stabilized by Cu(BDC) [115], HKUST-1 [116] and UiO-66 [117]. The macroporous monoliths obtained are characterized by an open-cell structure and very low densities (less than 0.2 g·m⁻³) [115,116]. Their porosity has been shown to depend on the MOF concentration, the amount of CO₂ introduced, and the crosslinking degree of the polymer. Monoliths prepared with low MOF concentrations (2–3 wt.% UiO-66 in the foam) have closed-cell structures in which the thickness of the PAM walls covers nearby pores, reducing the interconnectivity and specific surface area of the material. At higher MOF contents in contrast (5–7 wt %) [117], the foams contain 10–80 μm macropores connected by 0.5–25 μm windows [1]. Regarding the amount of CO₂ introduced, the pore sizes in HKUST-1-stabilized foams increased from 10–80 to 100–300 μm when the

amount of CO₂ used was reduced from 70 to 40 g [116]. In addition, decreasing the water/CO₂ mass ratio from 0.8 to 0.7 has been shown to reduce the resistance of Cu(BDC)/PAM materials from 2.2 to 1.5 MPa [115]. As for the degree of crosslinking finally, more highly crosslinked polymers lead to the formation of denser materials with smaller pores [115].

Macroporous monoliths can also be synthesized from water-in-oil emulsions with polymerization in the organic phase. ZIF-8 particles have been used (alongside Fe₂O₃ for magnetic functionalization) to stabilize water-in-oil emulsions with a polymeric continuous phase consisting of styrene, divinylbenzene and oleic acid as a swelling agent [118]. After polymerization and elimination of the internal phase, micro-meso-macroporous monoliths were obtained. ZIF-8 pores contribute to microporosity, mesopores with an average diameter of 38 nm result from neighboring ZIF-8 particles, and macropores formed by the emulsion droplets, whose size depends on the emulsification conditions as discussed above.

Pickering emulsions remain an interesting approach to produce hierarchically porous materials for the treatment of liquid effluents. The particles stabilize the droplets and form the walls of the monolith. The droplets themselves are larger than those in emulsions stabilized by organic surfactants, and therefore so are the macropores in the final monoliths. Furthermore, the continuous phase of the emulsions can be polymerized to improve the mechanical properties of the final material. Note however that although this has not been reported for Pickering emulsions, polymerization has been shown to cause pore blocking in surfactant-stabilized emulsions, as described above [97,98]. A simple way to overcome this problem should it arise would be to polymerize the continuous phase before adding the MOF particles.

Process	Techniques	MOFs	Porosity	Application	Ref.
Mechanical shaping	Extrusion/ Granulation	UiO-66	Micro-Mesoporous	Hydrogen storage	[30]
		MIL-53(Al)		Gas sorption	[34]
	3D printing	HKUST-1	Variable porosities	Multiple Applications	[39]
Sol-Gel process	Supramolecular templating	HKUST-1	Micro-Mesoporous	Bioengineering, Heterogeneous catalysis	[46]
	Metal Organic Gel (MOG)	MIL-100 (Fe)		Gas storage, Catalysis	[48]
	Designing membrane	HKUST-1	Micro-Meso-Macroporous	Small molecules separation	[60]
	Coating on monolith	MIL-101(Cr)		Heterogeneous catalysis	[59]
	Integration in polyHIPE structure	HKUST-1		Organic vapor adsorption, Dye removal	[67]
Zr-BDC-PUF			[68]		
Pickering Emulsion	microencapsulation/ Colloidosomes	ZIF-8	Micro-Meso-Macroporous	Drug/Molecule delivery	[107,108]
	Aerogel-type monoliths	HKUST-1		Dye/organic removal from water	[112]
		Zr-BDC-NO ₂ /GO		Fabrication of superstructures	[113]
	PolyHIPE monoliths	UiO-66		Dye removal	[111,114]

Table 1 : Summary table of the different MOF shaping techniques reported in this review.

7. Conclusion

The porosity, versatility and (chemical and thermal) stability of MOFs make them some of the most attractive porous materials for many applications. Compared with zeolites in particular, the range of possible developments with MOFs is almost limitless, which explains the dynamism of the field over the past two decades. Unfortunately, these exceptional capabilities have never made it out of research laboratories because the materials are usually produced as powders and at high cost (i.e. in very small, gram-scale amounts). Powder materials are difficult to use in most industrial applications so developing strategies to synthesize MOFs in bulk, handleable and hierarchically porous forms is one of the greatest challenges in MOF

research. Monolithic MOFs would be particularly valuable in fixed-bed catalysis or effluent treatment processes, where their large specific surface areas would boost exchange capacities and their interconnected macropores would improve fluid transfer and limit pressure drop.

The **Table 1** reports the different MOF shaping techniques we decided to highlight in this review. Most of methods developed so far to prepare MOFs in bulk form involve mechanical techniques (already developed for other materials or drugs). However, these methods can lead to crush the porosity of the pristine MOFs and destroy the MOF crystals, which reduce the efficiency of the material. The current focus is therefore on processes that preserve all the properties of pristine MOFs, for instance by inserting MOF particles into preformed macroporous supports or by growing them in situ. These processes are often complex however and high MOF loading is difficult to achieve.

From our point of view, the best strategy is perhaps to shape MOFs under mild conditions (as MOAs or MOXs) without any other binders to avoid pore blocking and preserve the original properties of the materials. An interconnected macroporous network can be formed by including a sacrificial template (such as emulsion droplets) in the synthesis. Unfortunately, the weak mechanical properties of these materials currently limit their industrial applicability. Binders, such as polymeric supports, can be added to strengthen the monoliths, the drawback being that adding binders typically leads to pore blocking. We are nevertheless convinced that these research avenues are worth pursuing to develop hierarchically porous MOFs monoliths suitable for industrial-scale effluent treatment. Moreover, we believe that, by this technic, it will be possible to increase the accessibility to active MOFs materials into the final structure. Therefore, it will reduce the quantity of necessary MOFs to present similar performances as well as the total cost of the material. This method seems also interesting in this way, compared to the other methods, by using no expensive devices and by reducing the number of synthetic steps.

Acknowledgments

This work was supported by the Occitanie Region and by the CEA through the VADEN project.

References

- [1] X.-Y. Yang, L.-H. Chen, Y. Li, J.C. Rooke, C. Sanchez, B.-L. Su, Hierarchically porous materials: synthesis strategies and structure design, *Chem. Soc. Rev.* 46 (2017) 481–558. <https://doi.org/10.1039/C6CS00829A>.
- [2] H. Furukawa, K.E. Cordova, M. O’Keeffe, O.M. Yaghi, The Chemistry and Applications of Metal-Organic Frameworks, *Science*. 341 (2013) 1230444–1230444. <https://doi.org/10.1126/science.1230444>.
- [3] H. Li, M. Eddaoudi, M. O’Keeffe, O.M. Yaghi, Design and synthesis of an exceptionally stable and highly porous metal-organic framework, *Nature*. 402 (1999) 276–279. <https://doi.org/10.1038/46248>.
- [4] L. Ma, C. Abney, W. Lin, Enantioselective catalysis with homochiral metal–organic frameworks, *Chem. Soc. Rev.* 38 (2009) 1248. <https://doi.org/10.1039/b807083k>.
- [5] R. Navarro Amador, L. Cirre, M. Carboni, D. Meyer, BTEX removal from aqueous solution with hydrophobic Zr metal organic frameworks, *J. Environ. Manage.* 214 (2018) 17–22. <https://doi.org/10.1016/j.jenvman.2018.02.097>.
- [6] E. Perez, M.-L. Andre, R. Navarro Amador, F. Hyvrard, J. Borrini, M. Carboni, D. Meyer, Recovery of metals from simulant spent lithium-ion battery as organophosphonate coordination polymers in aqueous media, *J. Hazard. Mater.* 317 (2016) 617–621. <https://doi.org/10.1016/j.jhazmat.2016.06.032>.
- [7] K.M.L. Taylor-Pashow, J. Della Rocca, Z. Xie, S. Tran, W. Lin, Postsynthetic Modifications of Iron-Carboxylate Nanoscale Metal–Organic Frameworks for Imaging and Drug Delivery, *J. Am. Chem. Soc.* 131 (2009) 14261–14263. <https://doi.org/10.1021/ja906198y>.
- [8] G. Genesio, J. Maynadié, M. Carboni, D. Meyer, Recent status on MOF thin films on transparent conductive oxides substrates (ITO or FTO), *New J. Chem.* 42 (2018) 2351–2363. <https://doi.org/10.1039/C7NJ03171H>.
- [9] Frameworks for commercial success, *Nat. Chem.* 8 (2016) 987–987. <https://doi.org/10.1038/nchem.2661>.
- [10] P. Silva, S.M.F. Vilela, J.P.C. Tomé, F.A. Almeida Paz, Multifunctional metal–organic frameworks: from academia to industrial applications, *Chem. Soc. Rev.* 44 (2015) 6774–6803. <https://doi.org/10.1039/C5CS00307E>.
- [11] S.L. James, C.J. Adams, C. Bolm, D. Braga, P. Collier, T. Friščić, F. Grepioni, K.D.M. Harris, G. Hyett, W. Jones, A. Krebs, J. Mack, L. Maini, A.G. Orpen, I.P. Parkin, W.C. Shearouse, J.W. Steed, D.C. Waddell, Mechanochemistry: opportunities for new and cleaner synthesis, *Chem Soc Rev.* 41 (2012) 413–447. <https://doi.org/10.1039/C1CS15171A>.

- [12] Y. Lv, X. Tan, F. Svec, Preparation and applications of monolithic structures containing metal-organic frameworks: Other Techniques, *J. Sep. Sci.* 40 (2017) 272–287. <https://doi.org/10.1002/jssc.201600423>.
- [13] A.U. Czaja, N. Trukhan, U. Müller, Industrial applications of metal–organic frameworks, *Chem. Soc. Rev.* 38 (2009) 1284. <https://doi.org/10.1039/b804680h>.
- [14] K. Sini, D. Bourgeois, M. Idouhar, M. Carboni, D. Meyer, Metal–organic framework sorbents for the removal of perfluorinated compounds in an aqueous environment, *New J. Chem.* 42 (2018) 17889–17894. <https://doi.org/10.1039/C8NJ03312A>.
- [15] K. Sini, D. Bourgeois, M. Idouhar, M. Carboni, D. Meyer, Metal-organic frameworks cavity size effect on the extraction of organic pollutants, *Mater. Lett.* 250 (2019) 92–95. <https://doi.org/10.1016/j.matlet.2019.04.113>.
- [16] M. Carboni, C.W. Abney, S. Liu, W. Lin, Highly porous and stable metal–organic frameworks for uranium extraction, *Chem. Sci.* 4 (2013) 2396. <https://doi.org/10.1039/c3sc50230a>.
- [17] M.I. Nandasiri, S.R. Jambovane, B.P. McGrail, H.T. Schaef, Satish.K. Nune, Adsorption, separation, and catalytic properties of densified metal-organic frameworks, *Coord. Chem. Rev.* 311 (2016) 38–52. <https://doi.org/10.1016/j.ccr.2015.12.004>.
- [18] P.J. Kitson, R.J. Marshall, D. Long, R.S. Forgan, L. Cronin, 3D Printed High-Throughput Hydrothermal Reactionware for Discovery, Optimization, and Scale-Up, *Angew. Chem. Int. Ed.* 53 (2014) 12723–12728. <https://doi.org/10.1002/anie.201402654>.
- [19] Y. Peng, V. Krungleviciute, I. Eryazici, J.T. Hupp, O.K. Farha, T. Yildirim, Methane Storage in Metal–Organic Frameworks: Current Records, Surprise Findings, and Challenges, *J. Am. Chem. Soc.* 135 (2013) 11887–11894. <https://doi.org/10.1021/ja4045289>.
- [20] A.I. Spjelkavik, Aarti, S. Divekar, T. Didriksen, R. Blom, Forming MOFs into Spheres by Use of Molecular Gastronomy Methods, *Chem. - Eur. J.* 20 (2014) 8973–8978. <https://doi.org/10.1002/chem.201402464>.
- [21] P. Küsgens, A. Zgaverdea, H.-G. Fritz, S. Siegle, S. Kaskel, Metal-Organic Frameworks in Monolithic Structures: Rapid Communications of the American Ceramic Society, *J. Am. Ceram. Soc.* 93 (2010) 2476–2479. <https://doi.org/10.1111/j.1551-2916.2010.03824.x>.
- [22] A. Carné-Sánchez, I. Imaz, M. Cano-Sarabia, D. MasPOCH, A spray-drying strategy for synthesis of nanoscale metal–organic frameworks and their assembly into hollow superstructures, *Nat. Chem.* 5 (2013) 203–211. <https://doi.org/10.1038/nchem.1569>.
- [23] Z. Lyu, G.J.H. Lim, R. Guo, Z. Kou, T. Wang, C. Guan, J. Ding, W. Chen, J. Wang, 3D-Printed MOF-Derived Hierarchically Porous Frameworks for Practical High-Energy Density Li-O₂ Batteries, *Adv. Funct. Mater.* 29 (2019) 1806658. <https://doi.org/10.1002/adfm.201806658>.
- [24] O. Shekhah, J. Liu, R.A. Fischer, Ch. Wöll, MOF thin films: existing and future applications, *Chem. Soc. Rev.* 40 (2011) 1081. <https://doi.org/10.1039/c0cs00147c>.
- [25] M.C. So, S. Jin, H.-J. Son, G.P. Wiederrecht, O.K. Farha, J.T. Hupp, Layer-by-Layer Fabrication of Oriented Porous Thin Films Based on Porphyrin-Containing Metal–Organic Frameworks, *J. Am. Chem. Soc.* 135 (2013) 15698–15701. <https://doi.org/10.1021/ja4078705>.
- [26] V. Chernikova, O. Shekhah, M. Eddaoudi, Advanced Fabrication Method for the Preparation of MOF Thin Films: Liquid-Phase Epitaxy Approach Meets Spin Coating Method, *ACS Appl. Mater. Interfaces.* 8 (2016) 20459–20464. <https://doi.org/10.1021/acsami.6b04701>.

- [27] D. Lenzen, P. Bendix, H. Reinsch, D. Fröhlich, H. Kummer, M. Möllers, P.P.C. Hügenell, R. Gläser, S. Henninger, N. Stock, Scalable Green Synthesis and Full-Scale Test of the Metal-Organic Framework CAU-10-H for Use in Adsorption-Driven Chillers, *Adv. Mater.* 30 (2018) 1705869. <https://doi.org/10.1002/adma.201705869>.
- [28] I. Hod, W. Bury, D.M. Karlin, P. Deria, C.-W. Kung, M.J. Katz, M. So, B. Klahr, D. Jin, Y.-W. Chung, T.W. Odom, O.K. Farha, J.T. Hupp, Directed Growth of Electroactive Metal-Organic Framework Thin Films Using Electrophoretic Deposition, *Adv. Mater.* 26 (2014) 6295–6300. <https://doi.org/10.1002/adma.201401940>.
- [29] S. Shanmugam, Granulation techniques and technologies: recent progresses, *BioImpacts.* 5 (2017) 55–63. <https://doi.org/10.15171/bi.2015.04>.
- [30] J. Ren, N.M. Musyoka, H.W. Langmi, A. Swartbooi, B.C. North, M. Mathe, A more efficient way to shape metal-organic framework (MOF) powder materials for hydrogen storage applications, *Int. J. Hydrog. Energy.* 40 (2015) 4617–4622. <https://doi.org/10.1016/j.ijhydene.2015.02.011>.
- [31] F. Akhtar, L. Andersson, S. Ogunwumi, N. Hedin, L. Bergström, Structuring adsorbents and catalysts by processing of porous powders, *J. Eur. Ceram. Soc.* 34 (2014) 1643–1666. <https://doi.org/10.1016/j.jeurceramsoc.2014.01.008>.
- [32] H. Wu, T. Yildirim, W. Zhou, Exceptional Mechanical Stability of Highly Porous Zirconium Metal–Organic Framework UiO-66 and Its Important Implications, *J. Phys. Chem. Lett.* 4 (2013) 925–930. <https://doi.org/10.1021/jz4002345>.
- [33] V. Finsy, L. Ma, L. Alaerts, D.E. De Vos, G.V. Baron, J.F.M. Denayer, Separation of CO₂/CH₄ mixtures with the MIL-53(Al) metal–organic framework, *Microporous Mesoporous Mater.* 120 (2009) 221–227. <https://doi.org/10.1016/j.micromeso.2008.11.007>.
- [34] M. Kriesten, J. Vargas Schmitz, J. Siegel, C.E. Smith, M. Kaspereit, M. Hartmann, Shaping of flexible Metal-Organic Frameworks: combining macroscopic stability and framework flexibility, *Eur. J. Inorg. Chem.* (2019). <https://doi.org/10.1002/ejic.201901100>.
- [35] S. Chaemchuen, K. Zhou, B. Mousavi, M. Ghadamyari, P.M. Heynderickx, S. Zhuiykov, M.S. Yusubov, F. Verpoort, Spray drying of zeolitic imidazolate frameworks: investigation of crystal formation and properties, *CrystEngComm.* 20 (2018) 3601–3608. <https://doi.org/10.1039/C8CE00392K>.
- [36] L. Garzón-Tovar, M. Cano-Sarabia, A. Carné-Sánchez, C. Carbonell, I. Imaz, D. MasPOCH, A spray-drying continuous-flow method for simultaneous synthesis and shaping of microspherical high nuclearity MOF beads, *React. Chem. Eng.* 1 (2016) 533–539. <https://doi.org/10.1039/C6RE00065G>.
- [37] J.A. Lewis, Direct Ink Writing of 3D Functional Materials, *Adv. Funct. Mater.* 16 (2006) 2193–2204. <https://doi.org/10.1002/adfm.200600434>.
- [38] M. Bible, M. Sefa, J.A. Fedchak, J. Scherschligt, B. Natarajan, Z. Ahmed, M.R. Hartings, 3D-Printed Acrylonitrile Butadiene Styrene-Metal Organic Framework Composite Materials and Their Gas Storage Properties, *3D Print. Addit. Manuf.* 5 (2018) 63–72. <https://doi.org/10.1089/3dp.2017.0067>.
- [39] G.J.H. Lim, Y. Wu, B.B. Shah, J.J. Koh, C.K. Liu, D. Zhao, A.K. Cheetham, J. Wang, J. Ding, 3D-Printing of Pure Metal–Organic Framework Monoliths, *ACS Mater. Lett.* 1 (2019) 147–153. <https://doi.org/10.1021/acsmaterialslett.9b00069>.
- [40] M. Eddaoudi, Systematic Design of Pore Size and Functionality in Isoreticular MOFs and Their Application in Methane Storage, *Science.* 295 (2002) 469–472. <https://doi.org/10.1126/science.1067208>.

- [41] H. Furukawa, N. Ko, Y.B. Go, N. Aratani, S.B. Choi, E. Choi, A.O. Yazaydin, R.Q. Snurr, M. O’Keeffe, J. Kim, O.M. Yaghi, Ultrahigh Porosity in Metal-Organic Frameworks, *Science*. 329 (2010) 424–428. <https://doi.org/10.1126/science.1192160>.
- [42] J.-R. Li, R.J. Kuppler, H.-C. Zhou, Selective gas adsorption and separation in metal–organic frameworks, *Chem. Soc. Rev.* 38 (2009) 1477. <https://doi.org/10.1039/b802426j>.
- [43] Q. Huo, D.I. Margolese, U. Ciesla, P. Feng, T.E. Gier, P. Sieger, R. Leon, P.M. Petroff, F. Schüth, G.D. Stucky, Generalized synthesis of periodic surfactant/inorganic composite materials, *Nature*. 368 (1994) 317–321. <https://doi.org/10.1038/368317a0>.
- [44] C.T. Kresge, M.E. Leonowicz, W.J. Roth, J.C. Vartuli, J.S. Beck, Ordered mesoporous molecular sieves synthesized by a liquid-crystal template mechanism, *Nature*. 359 (1992) 710–712. <https://doi.org/10.1038/359710a0>.
- [45] S. Hartmann, D. Brandhuber, N. Hüsing, Glycol-Modified Silanes: Novel Possibilities for the Synthesis of Hierarchically Organized (Hybrid) Porous Materials, *Acc. Chem. Res.* 40 (2007) 885–894. <https://doi.org/10.1021/ar6000318>.
- [46] L.-G. Qiu, T. Xu, Z.-Q. Li, W. Wang, Y. Wu, X. Jiang, X.-Y. Tian, L.-D. Zhang, Hierarchically Micro- and Mesoporous Metal-Organic Frameworks with Tunable Porosity, *Angew. Chem. Int. Ed.* 47 (2008) 9487–9491. <https://doi.org/10.1002/anie.200803640>.
- [47] N.Ch. Das, H. Cao, H. Kaiser, G.T. Warren, J.R. Gladden, P.E. Sokol, Shape and Size of Highly Concentrated Micelles in CTAB/NaSal Solutions by Small Angle Neutron Scattering (SANS), *Langmuir*. 28 (2012) 11962–11968. <https://doi.org/10.1021/la2022598>.
- [48] M.R. Lohe, M. Rose, S. Kaskel, Metal–organic framework (MOF) aerogels with high micro- and macroporosity, *Chem. Commun.* (2009) 6056. <https://doi.org/10.1039/b910175f>.
- [49] A.P. Nelson, O.K. Farha, K.L. Mulfort, J.T. Hupp, Supercritical Processing as a Route to High Internal Surface Areas and Permanent Microporosity in Metal–Organic Framework Materials, *J. Am. Chem. Soc.* 131 (2009) 458–460. <https://doi.org/10.1021/ja808853q>.
- [50] S.K. Nune, P.K. Thallapally, B.P. McGrail, Metal organic gels (MOGs): a new class of sorbents for CO₂ separation applications, *J. Mater. Chem.* 20 (2010) 7623. <https://doi.org/10.1039/c0jm01907k>.
- [51] S.M.F. Vilela, P. Salcedo-Abraira, L. Micheron, E.L. Solla, P.G. Yot, P. Horcajada, A robust monolithic metal-organic framework with hierarchical porosity, *Chem. Commun. Camb. Engl.* 54 (2018) 13088–13091. <https://doi.org/10.1039/c8cc07252c>.
- [52] L. Li, S. Xiang, S. Cao, J. Zhang, G. Ouyang, L. Chen, C.-Y. Su, A synthetic route to ultralight hierarchically micro/mesoporous Al(III)-carboxylate metal-organic aerogels, *Nat. Commun.* 4 (2013). <https://doi.org/10.1038/ncomms2757>.
- [53] W. Xia, X. Zhang, L. Xu, Y. Wang, J. Lin, R. Zou, Facile and economical synthesis of metal–organic framework MIL-100(Al) gels for high efficiency removal of microcystin-LR, *RSC Adv.* 3 (2013) 11007. <https://doi.org/10.1039/c3ra40741a>.
- [54] B. Bueken, N. Van Velthoven, T. Willhammar, T. Stassin, I. Stassen, D.A. Keen, G.V. Baron, J.F.M. Denayer, R. Ameloot, S. Bals, D. De Vos, T.D. Bennett, Gel-based morphological design of zirconium metal-organic frameworks, *Chem. Sci.* 8 (2017) 3939–3948. <https://doi.org/10.1039/c6sc05602d>.
- [55] A. Mahmood, W. Xia, N. Mahmood, Q. Wang, R. Zou, Hierarchical Heteroaggregation of Binary Metal-Organic Gels with Tunable Porosity and Mixed Valence Metal Sites for Removal of Dyes in Water, *Sci. Rep.* 5 (2015). <https://doi.org/10.1038/srep10556>.

- [56] H.B. Aiyappa, S. Saha, B. Garai, J. Thote, S. Kurungot, R. Banerjee, A Distinctive PdCl₂-Mediated Transformation of Fe-Based Metallogels into Metal–Organic Frameworks, *Cryst. Growth Des.* 14 (2014) 3434–3437. <https://doi.org/10.1021/cg500368q>.
- [57] T. Tian, Z. Zeng, D. Vulpe, M.E. Casco, G. Divitini, P.A. Midgley, J. Silvestre-Albero, J.-C. Tan, P.Z. Moghadam, D. Fairen-Jimenez, A sol-gel monolithic metal-organic framework with enhanced methane uptake, *Nat. Mater.* 17 (2018) 174–179. <https://doi.org/10.1038/NMAT5050>.
- [58] B.M. Connolly, M. Aragonés-Anglada, J. Gandara-Loe, N.A. Danaf, D.C. Lamb, J.P. Mehta, D. Vulpe, S. Wuttke, J. Silvestre-Albero, P.Z. Moghadam, A.E.H. Wheatley, D. Fairen-Jimenez, Tuning porosity in macroscopic monolithic metal-organic frameworks for exceptional natural gas storage, *Nat. Commun.* 10 (2019) 2345. <https://doi.org/10.1038/s41467-019-10185-1>.
- [59] E.V. Ramos-Fernandez, M. Garcia-Domingos, J. Juan-Alcañiz, J. Gascon, F. Kapteijn, MOFs meet monoliths: Hierarchical structuring metal organic framework catalysts, *Appl. Catal. Gen.* 391 (2011) 261–267. <https://doi.org/10.1016/j.apcata.2010.05.019>.
- [60] J. Nan, X. Dong, W. Wang, W. Jin, N. Xu, Step-by-Step Seeding Procedure for Preparing HKUST-1 Membrane on Porous α -Alumina Support, *Langmuir.* 27 (2011) 4309–4312. <https://doi.org/10.1021/la200103w>.
- [61] D. Qian, C. Lei, G.-P. Hao, W.-C. Li, A.-H. Lu, Synthesis of Hierarchical Porous Carbon Monoliths with Incorporated Metal–Organic Frameworks for Enhancing Volumetric Based CO₂ Capture Capability, *ACS Appl. Mater. Interfaces.* 4 (2012) 6125–6132. <https://doi.org/10.1021/am301772k>.
- [62] U. Betke, S. Proemmel, S. Rannabauer, A. Lieb, M. Scheffler, F. Scheffler, Silane functionalized open-celled ceramic foams as support structure in metal organic framework composite materials, *Microporous Mesoporous Mater.* 239 (2017) 209–220. <https://doi.org/10.1016/j.micromeso.2016.10.011>.
- [63] A. Sachse, R. Ameloot, B. Coq, F. Fajula, B. Coasne, D. De Vos, A. Galarneau, In situ synthesis of Cu–BTC (HKUST-1) in macro-/mesoporous silica monoliths for continuous flow catalysis, *Chem. Commun.* 48 (2012) 4749. <https://doi.org/10.1039/c2cc17190b>.
- [64] G.-Q. Song, Y.-X. Lu, Q. Zhang, F. Wang, X.-K. Ma, X.-F. Huang, Z.-H. Zhang, Porous Cu–BTC silica monoliths as efficient heterogeneous catalysts for the selective oxidation of alkylbenzenes, *RSC Adv.* 4 (2014) 30221–30224. <https://doi.org/10.1039/C4RA04076G>.
- [65] A. Galarneau, A. Sachse, B. Said, C.-H. Pelisson, P. Boscaro, N. Brun, L. Courtheoux, N. Olivi-Tran, B. Coasne, F. Fajula, Hierarchical porous silica monoliths: A novel class of microreactors for process intensification in catalysis and adsorption, *Comptes Rendus Chim.* 19 (2016) 231–247. <https://doi.org/10.1016/j.crci.2015.05.017>.
- [66] M.G. Schwab, I. Senkowska, M. Rose, M. Koch, J. Pahnke, G. Jonschker, S. Kaskel, MOF@PolyHIPEs, *Adv. Eng. Mater.* 10 (2008) 1151–1155. <https://doi.org/10.1002/adem.200800189>.
- [67] M.L. Pinto, S. Dias, J. Pires, Composite MOF Foams: The Example of UiO-66/Polyurethane, *ACS Appl. Mater. Interfaces.* 5 (2013) 2360–2363. <https://doi.org/10.1021/am303089g>.
- [68] J. Li, J.-L. Gong, G.-M. Zeng, P. Zhang, B. Song, W.-C. Cao, H.-Y. Liu, S.-Y. Huan, Zirconium-based metal organic frameworks loaded on polyurethane foam membrane for simultaneous removal of dyes with different charges, *J. Colloid Interface Sci.* 527 (2018) 267–279. <https://doi.org/10.1016/j.jcis.2018.05.028>.
- [69] L. Wen, A. Gao, Y. Cao, F. Svec, T. Tan, Y. Lv, Layer-by-Layer Assembly of Metal–Organic Frameworks in Macroporous Polymer Monolith and Their Use for Enzyme

- Immobilization, *Macromol. Rapid Commun.* 37 (2016) 551–557.
<https://doi.org/10.1002/marc.201500705>.
- [70] X. Ma, Y. Lou, X.-B. Chen, Z. Shi, Y. Xu, Multifunctional flexible composite aerogels constructed through in-situ growth of metal-organic framework nanoparticles on bacterial cellulose, *Chem. Eng. J.* 356 (2019) 227–235.
<https://doi.org/10.1016/j.cej.2018.09.034>.
- [71] L. Valencia, H.N. Abdelhamid, Nanocellulose leaf-like zeolitic imidazolate framework (ZIF-L) foams for selective capture of carbon dioxide, *Carbohydr. Polym.* 213 (2019) 338–345. <https://doi.org/10.1016/j.carbpol.2019.03.011>.
- [72] S. Aguado, J. Canivet, D. Farrusseng, Engineering structured MOF at nano and macroscales for catalysis and separation, *J. Mater. Chem.* 21 (2011) 7582.
<https://doi.org/10.1039/c1jm10787a>.
- [73] S. Lawson, A. Hajari, A.A. Rownaghi, F. Rezaei, MOF immobilization on the surface of polymer-cordierite composite monoliths through in-situ crystal growth, *Sep. Purif. Technol.* 183 (2017) 173–180. <https://doi.org/10.1016/j.seppur.2017.03.072>.
- [74] S.R. Venna, M.A. Carreon, Highly Permeable Zeolite Imidazolate Framework-8 Membranes for CO₂/CH₄ Separation, *J. Am. Chem. Soc.* 132 (2010) 76–78.
<https://doi.org/10.1021/ja909263x>.
- [75] Z. Ulker, I. Erucar, S. Keskin, C. Erkey, Novel nanostructured composites of silica aerogels with a metal organic framework, *Microporous Mesoporous Mater.* 170 (2013) 352–358. <https://doi.org/10.1016/j.micromeso.2012.11.040>.
- [76] A. Prabhu, A. Al Shoaibi, C. Srinivasakannan, Preparation and characterization of silica aerogel-ZIF-8 hybrid materials, *Mater. Lett.* 146 (2015) 43–46.
<https://doi.org/10.1016/j.matlet.2015.01.156>.
- [77] A.L. Nuzhdin, A.S. Shalygin, E.A. Artiukha, A.M. Chibiryaev, G.A. Bukhtiyarova, O.N. Martyanov, HKUST-1 silica aerogel composites: novel materials for the separation of saturated and unsaturated hydrocarbons by conventional liquid chromatography, *RSC Adv.* 6 (2016) 62501–62507. <https://doi.org/10.1039/C6RA06522H>.
- [78] M. Wickenheisser, A. Herbst, R. Tannert, B. Milow, C. Janiak, Hierarchical MOF-xerogel monolith composites from embedding MIL-100(Fe,Cr) and MIL-101(Cr) in resorcinol-formaldehyde xerogels for water adsorption applications, *Microporous Mesoporous Mater.* 215 (2015) 143–153.
<https://doi.org/10.1016/j.micromeso.2015.05.017>.
- [79] A.L. Nuzhdin, A.S. Shalygin, E.A. Artiukha, A.M. Chibiryaev, G.A. Bukhtiyarova, O.N. Martyanov, HKUST-1 silica aerogel composites: novel materials for the separation of saturated and unsaturated hydrocarbons by conventional liquid chromatography, *RSC Adv.* 6 (2016) 62501–62507. <https://doi.org/10.1039/c6ra06522h>.
- [80] Q. Fu, L. Wen, L. Zhang, X. Chen, D. Pun, A. Ahmed, Y. Yang, H. Zhang, Preparation of Ice-Templated MOF–Polymer Composite Monoliths and Their Application for Wastewater Treatment with High Capacity and Easy Recycling, *ACS Appl. Mater. Interfaces.* 9 (2017) 33979–33988. <https://doi.org/10.1021/acsami.7b10872>.
- [81] H. Zhu, X. Yang, E.D. Cranston, S. Zhu, Flexible and Porous Nanocellulose Aerogels with High Loadings of Metal-Organic-Framework Particles for Separations Applications, *Adv. Mater.* 28 (2016) 7652–7657.
<https://doi.org/10.1002/adma.201601351>.
- [82] Z. Wang, L. Song, Y. Wang, X.-F. Zhang, D. Hao, Y. Feng, J. Yao, Lightweight UiO-66/cellulose aerogels constructed through self-crosslinking strategy for adsorption applications, *Chem. Eng. J.* 371 (2019) 138–144.
<https://doi.org/10.1016/j.cej.2019.04.022>.

- [83] H. Zhu, X. Yang, E.D. Cranston, S. Zhu, Flexible and Porous Nanocellulose Aerogels with High Loadings of Metal-Organic-Framework Particles for Separations Applications, *Adv. Mater.* 28 (2016) 7652–7657. <https://doi.org/10.1002/adma.201601351>.
- [84] K. Nakanishi, Pore Structure Control of Silica Gels Based on Phase Separation, *J. Porous Mater.* 4 (1997) 67–112. <https://doi.org/10.1023/A:1009627216939>.
- [85] Y. Tokudome, K. Fujita, K. Nakanishi, K. Miura, K. Hirao, Synthesis of Monolithic Al₂O₃ with Well-Defined Macropores and Mesoporous Skeletons via the Sol–Gel Process Accompanied by Phase Separation, *Chem. Mater.* 19 (2007) 3393–3398. <https://doi.org/10.1021/cm063051p>.
- [86] J. Konishi, K. Fujita, K. Nakanishi, K. Hirao, Monolithic TiO₂ with Controlled Multiscale Porosity via a Template-Free Sol–Gel Process Accompanied by Phase Separation, *Chem. Mater.* 18 (2006) 6069–6074. <https://doi.org/10.1021/cm0617485>.
- [87] A. Sachse, A. Galarneau, F. Di Renzo, F. Fajula, B. Coq, Synthesis of Zeolite Monoliths for Flow Continuous Processes. The Case of Sodalite as a Basic Catalyst, *Chem. Mater.* 22 (2010) 4123–4125. <https://doi.org/10.1021/cm1014064>.
- [88] B. Said, A. Grandjean, Y. Barre, F. Tancret, F. Fajula, A. Galarneau, LTA zeolite monoliths with hierarchical trimodal porosity as highly efficient microreactors for strontium capture in continuous flow, *Microporous Mesoporous Mater.* 232 (2016) 39–52. <https://doi.org/10.1016/j.micromeso.2016.05.036>.
- [89] C. Cabaud, Y. Barré, L. De Windt, S. Gill, E. Dooryhée, M.P. Moloney, N. Massoni, A. Grandjean, Removing Cs within a continuous flow set-up by an ionic exchanger material transformable into a final waste form, *Adsorption.* 25 (2019) 765–771. <https://doi.org/10.1007/s10450-019-00040-6>.
- [90] N. Moitra, S. Fukumoto, J. Reboul, K. Sumida, Y. Zhu, K. Nakanishi, S. Furukawa, S. Kitagawa, K. Kanamori, Mechanically stable, hierarchically porous Cu-3(btc)(2) (HKUST-1) monoliths via direct conversion of copper(II) hydroxide-based monoliths, *Chem. Commun.* 51 (2015) 3511–3514. <https://doi.org/10.1039/c4cc09694k>.
- [91] N. Parsazadeh, F. Yousefi, M. Ghaedi, K. Dashtian, F. Borousan, Preparation and characterization of monoliths HKUST-1 MOF *via* straightforward conversion of Cu(OH)₂-based monoliths and its application for wastewater treatment: artificial neural network and central composite design modeling, *New J. Chem.* 42 (2018) 10327–10336. <https://doi.org/10.1039/C8NJ01067F>.
- [92] E. Hastürk, C. Schlüsener, J. Quodbach, A. Schmitz, C. Janiak, Shaping of metal-organic frameworks into mechanically stable monoliths with poly(vinyl alcohol) by phase separation technique, *Microporous Mesoporous Mater.* 280 (2019) 277–287. <https://doi.org/10.1016/j.micromeso.2019.02.011>.
- [93] M. Destribats, M. Wolfs, F. Pinaud, V. Lapeyre, E. Sellier, V. Schmitt, V. Ravaine, Pickering Emulsions Stabilized by Soft Microgels: Influence of the Emulsification Process on Particle Interfacial Organization and Emulsion Properties, *Langmuir.* 29 (2013) 12367–12374. <https://doi.org/10.1021/la402921b>.
- [94] A. Roucher, V. Schmitt, J.-L. Blin, R. Backov, Sol–gel process and complex fluids: sculpting porous matter at various lengths scales towards the Si(HIPE), Si(PHIPE), and SBA-15-Si(HIPE) series, *J. Sol-Gel Sci. Technol.* 90 (2019) 95–104. <https://doi.org/10.1007/s10971-018-4794-8>.
- [95] L. Lei, Q. Zhang, S. Shi, S. Zhu, Highly Porous Poly(high internal phase emulsion) Membranes with “Open-Cell” Structure and CO₂-Switchable Wettability Used for Controlled Oil/Water Separation, *Langmuir.* 33 (2017) 11936–11944. <https://doi.org/10.1021/acs.langmuir.7b02539>.

- [96] K.M. Althubeiti, T.S. Horozov, Efficient preparation of macroporous poly(methyl methacrylate) materials from high internal phase emulsion templates, *React. Funct. Polym.* 142 (2019) 207–212. <https://doi.org/10.1016/j.reactfunctpolym.2019.06.015>.
- [97] M. Wickenheisser, C. Janiak, Hierarchical embedding of micro-mesoporous MIL-101(Cr) in macroporous poly(2-hydroxyethyl methacrylate) high internal phase emulsions with monolithic shape for vapor adsorption applications, *Microporous Mesoporous Mater.* 204 (2015) 242–250. <https://doi.org/10.1016/j.micromeso.2014.11.025>.
- [98] M. Wickenheisser, T. Paul, C. Janiak, Prospects of monolithic MIL-MOF@poly(NIPAM)HIPE composites as water sorption materials, *Microporous Mesoporous Mater.* 220 (2016) 258–269. <https://doi.org/10.1016/j.micromeso.2015.09.008>.
- [99] R. Aveyard, B.P. Binks, J.H. Clint, Emulsions stabilised solely by colloidal particles, *Adv. Colloid Interface Sci.* 100–102 (2003) 503–546. [https://doi.org/10.1016/S0001-8686\(02\)00069-6](https://doi.org/10.1016/S0001-8686(02)00069-6).
- [100] B.P. Binks, Particles as surfactants—similarities and differences, *Curr. Opin. Colloid Interface Sci.* 7 (2002) 21–41. [https://doi.org/10.1016/S1359-0294\(02\)00008-0](https://doi.org/10.1016/S1359-0294(02)00008-0).
- [101] B.P. Binks, S.O. Lumsdon, Influence of Particle Wettability on the Type and Stability of Surfactant-Free Emulsions[†], *Langmuir.* 16 (2000) 8622–8631. <https://doi.org/10.1021/la000189s>.
- [102] B.P. Binks, Colloidal particles at liquid interfaces, *Phys. Chem. Chem. Phys.* 9 (2007) 6298. <https://doi.org/10.1039/b716587k>.
- [103] M. Liu, L. Tie, J. Li, Y. Hou, Z. Guo, Underoil superhydrophilic surfaces: water adsorption in metal–organic frameworks, *J. Mater. Chem. A.* 6 (2018) 1692–1699. <https://doi.org/10.1039/C7TA09711E>.
- [104] B. Xiao, Q. Yuan, R.A. Williams, Exceptional function of nanoporous metal organic framework particles in emulsion stabilisation, *Chem. Commun.* 49 (2013) 8208. <https://doi.org/10.1039/c3cc43689f>.
- [105] C. Liu, J. Zhang, L. Zheng, J. Zhang, X. Sang, X. Kang, B. Zhang, T. Luo, X. Tan, B. Han, Metal-Organic Framework for Emulsifying Carbon Dioxide and Water, *Angew. Chem. Int. Ed.* 55 (2016) 11372–11376. <https://doi.org/10.1002/anie.201602150>.
- [106] Z. Li, J. Zhang, T. Luo, X. Tan, C. Liu, X. Sang, X. Ma, B. Han, G. Yang, High internal ionic liquid phase emulsion stabilized by metal–organic frameworks, *Soft Matter.* 12 (2016) 8841–8846. <https://doi.org/10.1039/C6SM01610C>.
- [107] J. Huo, M. Marcello, A. Garai, D. Bradshaw, MOF-Polymer Composite Microcapsules Derived from Pickering Emulsions, *Adv. Mater.* 25 (2013) 2717–2722. <https://doi.org/10.1002/adma.201204913>.
- [108] W. Liu, Y. Zhao, C. Zeng, C. Wang, C.A. Serra, L. Zhang, Microfluidic preparation of yolk/shell ZIF-8/alginate hybrid microcapsules from Pickering emulsion, *Chem. Eng. J.* 307 (2017) 408–417. <https://doi.org/10.1016/j.cej.2016.08.097>.
- [109] H. Zhu, Q. Zhang, S. Zhu, MOFsomes via Transient Pickering Emulsion Template, *Adv. Mater. Interfaces.* 3 (2016) 1600294. <https://doi.org/10.1002/admi.201600294>.
- [110] F. Zhang, X. Sang, X. Tan, C. Liu, J. Zhang, T. Luo, L. Liu, B. Han, G. Yang, B.P. Binks, Converting Metal–Organic Framework Particles from Hydrophilic to Hydrophobic by an Interfacial Assembling Route, *Langmuir.* 33 (2017) 12427–12433. <https://doi.org/10.1021/acs.langmuir.7b02365>.
- [111] H. Zhu, Q. Zhang, S. Zhu, Assembly of a Metal-Organic Framework into 3 D Hierarchical Porous Monoliths Using a Pickering High Internal Phase Emulsion

- Template, Chem. - Eur. J. 22 (2016) 8751–8755.
<https://doi.org/10.1002/chem.201600313>.
- [112] B. Zhang, J. Zhang, C. Liu, L. Peng, X. Sang, B. Han, X. Ma, T. Luo, X. Tan, G. Yang, High-internal-phase emulsions stabilized by metal-organic frameworks and derivation of ultralight metal-organic aerogels, Sci. Rep. 6 (2016) 21401.
<https://doi.org/10.1038/srep21401>.
- [113] F. Zhang, L. Liu, X. Tan, X. Sang, J. Zhang, C. Liu, B. Zhang, B. Han, G. Yang, Pickering emulsions stabilized by a metal–organic framework (MOF) and graphene oxide (GO) for producing MOF/GO composites, Soft Matter. 13 (2017) 7365–7370.
<https://doi.org/10.1039/C7SM01567D>.
- [114] J. Wang, H. Zhu, B.-G. Li, S. Zhu, Interconnected Porous Monolith Prepared via UiO-66 Stabilized Pickering High Internal Phase Emulsion Template, Chem. - Eur. J. 24 (2018) 16426–16431. <https://doi.org/10.1002/chem.201803628>.
- [115] Z. Yang, L. Cao, J. Li, J. Lin, J. Wang, Facile synthesis of Cu-BDC/Poly(N-methylol acrylamide) HIPE monoliths via CO₂-in-water Emulsion stabilized by metal-organic framework, Polymer. 153 (2018) 17–23. <https://doi.org/10.1016/j.polymer.2018.07.085>.
- [116] Y. Yang, L. Cao, J. Li, Y. Dong, J. Wang, High-Performance Composite Monolith Synthesized via HKUST-1 Stabilized HIPEs and Its Adsorptive Properties, Macromol. Mater. Eng. 303 (2018) 1800426. <https://doi.org/10.1002/mame.201800426>.
- [117] Y. Dong, L. Cao, J. Li, Y. Yang, J. Wang, Facile preparation of UiO-66 /PAM monoliths *via* CO₂ -in-water HIPEs and their applications, RSC Adv. 8 (2018) 32358–32367. <https://doi.org/10.1039/C8RA05809A>.
- [118] P. Jin, W. Tan, J. Huo, T. Liu, Y. Liang, S. Wang, D. Bradshaw, Hierarchically porous MOF/polymer composites *via* interfacial nanoassembly and emulsion polymerization, J. Mater. Chem. A. 6 (2018) 20473–20479. <https://doi.org/10.1039/C8TA06766J>.

